Article

Numerical Simulations of the Oscillating Second-Grade Fluid through a Rectangular Cross Duct with Fractional Constitution Relationship

Bo Zhang [1], Lin Liu [1,2,*], Siyu Chen [1], Sen Zhang [1], Lang Liu [1], Libo Feng [3] , Jing Zhu [1], Jiangshan Zhang [2] and Liancun Zheng [1]

1   School of Mathematics and Physics, University of Science and Technology Beijing, Beijing 100083, China
2   State Key Laboratory of Advanced Metallurgy, University of Science and Technology Beijing, Beijing 100083, China
3   School of Mathematical Sciences, Queensland University of Technology, Brisbane, QLD 4001, Australia
*   Correspondence: liulin@ustb.edu.cn

Abstract: An oscillating second-grade fluid through a rectangular cross duct is studied. A traditional integer time derivative in the kinematic tensors is substituted by a fractional operator that considers the memory characteristics. To treat the fractional governing equation, an analytical method was obtained. To analyze the impact of the parameters more intuitively, the difference method was applied to determine the numerical expression and draw with the help of computer simulation. To reduce the cost of the amount of computation and storage, a fast scheme was proposed, one which can greatly improve the calculation speed. To verify the correctness of the difference scheme, the contrast between the numerical expression and the exact expression—constructed by introducing a source term—was given and the superiority of the fast scheme is discussed. Furthermore, the influences of the involved parameters, including the parameter of retardation time, fractional parameter, magnetic parameter, and oscillatory frequency parameter, on the distributions of velocity and shear force at the wall surface with oscillatory flow are analyzed in detail.

Keywords: second-grade fluid; rectangular duct; constitution relationship; fractional derivative; fast algorithms

1. Introduction

The flow of fluid has widespread applications, including in aerospace, biomedicine, oil exploitation etc. The classical fluid model is the Newtonian fluid in which the stress tensor and the kinematic tensor have a linear relationship. It has a limitation in so far that it can only describe most pure liquids such as water and alcohol. In addition to the fluids listed, most fluids are non-Newtonian whose characteristics have many properties that different from those of Newtonian ones [1]. Studying the flow mechanism has great significance. There are many types of non-Newtonian fluids and this paper studies the second-grade fluid [2–4], in which the shear force is characterized by the stretching tensor and the Rivlin–Ericksen tensors.

Due to the special description of the constitution relationship, the second-grade fluid has its own unique properties. In order to better discover its flow mechanism, the usual method is to consider the flow through simple models. The common categories for this include the flow on semi-infinite plates [5,6], two parallel infinitely long plates [7], the flow in pipes or ducts [8], or the flow in a circular tube [9]. Non-Newtonian fluids in rectangular channels have gained special interest for the engineering applications such as in magnetohydrodynamic generators and marine mechanical equipment, interest which has helped us to study the flow characteristics in depth [10]. Studying second-grade fluid in a rectangular cross duct has important research significance and application value. Erdoğan and İmrak [11] were the first scholars to study the unsteady motion of second-grade fluid

through a rectangular cross duct with the influences of the side walls. It has been further studied by many scholars. Considering heat transfer with relaxation time, Alamri et al. [12] analyzed particle diffusion in the flow of second-grade fluid and discussed the effects of the involved parameters on the profile graphically. Bernard [13] studied a three-dimensional second-grade fluid with a tangential boundary condition in a polyhedron. By comparing with the stress of the Newtonian fluid at the initial time, Erdoğan and İmrak [14] considered the motion properties of second-grade fluid driven by the impulsive motion or sudden pressure gradient. The comparison of the stress at the start time between the Newtonian fluid and the second-grade fluid was discussed. Furthermore, the influence of the magnetic field has important research significance. It has been applied to the Maxwell fluid [15], Oldroyd-B fluid [16] et al., but it has fewer studies on the second-grade fluid.

Besides, many situations consider the steady-state motion of the second-grade fluid for simplicity. However, for the practical situation, the velocity field produced by the flow should vary with time due to the complexity of the fluid flow. The unsteady state has more research significance for the second-grade fluid with the condition that the time derivative in the constitutional relationship is integral to considering the local characteristics. With further research, it has been found that the fractional model has gained support for its memory characteristic [17]. At present, the fractional operators have been applied in many viscoelastic fluids, such as the Maxwell model [18], Oldroyd-B model [19], Burgers' model [20] et al. For the fractional second-grade fluid, the constitution relationship has a similar form with the viscoelastic fluid, namely, they all have the fractional material derivative term. The application of fractional operator on the motion of second-grade fluid has been analyzed by Tan and Xu [21], Bazhlekova et al. [22], Kan and Wang [23], Li et al. [24] et al. For flow driven by a special form of oscillatory pressure, it has been widely applied in the motions in an isosceles right triangle tube with Maxwell fluid [25], in a straight rectangular duct with the second-grade fluid [26], in a cylindrical domain with the Oldroyd-B fluid [27], and in cylindrical domains with the fractional Burgers fluid [28]. To the best of the authors' knowledge, the two-dimensional flow of second-grade fluid in rectangular ducts driven by oscillatory pressure and considering a magnetic field has not been considered in the literature so far.

There are many methods to solve the governing equation [29–31]. For the treatment of the fractional second-grade fluid, the traditional method is to apply the integral transform method to obtain an analytical solution [27,32,33], with the paradox that the principle of causality causing the initial conditions is a non-rigorous enforcement. In other words, these treatments for the start-up flow proposed by Christov [34,35] are incorrect. There are many numerical methods [36] that can solve the fractional governing equation and the numerical difference method has been applied to solve the corresponding mathematical problem correctly.

The governing equation subject to the fractional second-grade constitutive relationship is solved numerically. The difference is that the integer term has mature calculation methods, while the key is to treat the fractional derivative. The classical method is to choose the L1 scheme [37] to approximate it, though it is limited by the huge amount of computation and storage required for long-term numerical simulation, since the Caputo derivative depends on historical information. This is an urgent problem to be solved at present. Using exponential functions to approximate the Abel kernel function of Caputo derivatives, the fast algorithm [38] has been developed. The main idea is to reduce the number of iterations by constructing a recurrent relationship. At each time step, the convolution containing the exponential kernel is calculated in $O(1)$ time. Then the computational amount $O(N^2)$ and storage $O(N)$ for the direct L1-algorithm reduces to $O(N \log_2 N)$ and $O(\log_2 N)$ for the fast algorithm, respectively. This has been applied to treat fractional diffusion models [39], multi-term fractional sub-diffusion models [40], wave models [41] and the variable co-efficient fractional diffusion wave models [42]. According to the numerical results, the analyses are discussed and are detailed by graphical illustration.

The paper's outline is given as follows. The derivation of the mathematical model of the second-grade fluid over a rectangular duct with an infinite length and which is caused by a various pressure gradient is given in Section 2. The exact expression for describing the second-grade fluid is deduced in Section 3. Section 4 gives the numerical difference scheme of the formulated governing equation and the analyses of the solvability, stability and convergence are proven in Section 5. Section 6 gives the fast evolution of the difference scheme. Section 7 gives the comparison between the numerical expression and the exact expression. Furthermore, the influences of the relevant parameters on the transfer mechanism of the velocity field and the shear force at the wall surface are also analyzed. The conclusions are summarized in Section 8.

2. The Derivation of the Mathematical Model

Consider the motions of an incompressible second-grade fluid. The laminar flow in a straight duct with infinite length and the rectangular cross-section is considered and the flow is controlled by pressure gradient with time/space oscillations. As shown in Figure 1, the width and height of the rectangular section are $2a$ and $2b$. The center in the cross-section is defined as the origin and the boundaries along x direction and y direction are at the positions $x = \pm a$ and $y = \pm b$ while $z \in [0, +\infty)$ along z direction. For simplicity, the body forces are neglected in this paper.
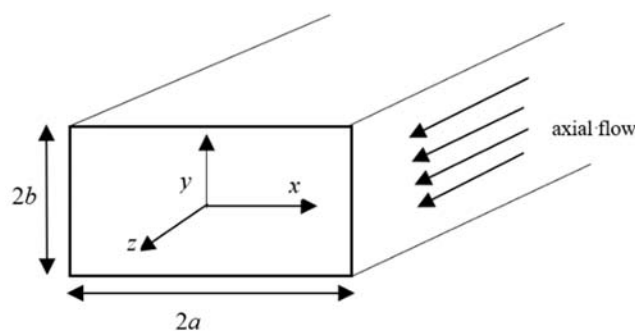
Figure 1. The motion of second-grade fluid in a rectangular cross duct.

The continuity equation is given as

$$\nabla \cdot V = 0, \tag{1}$$

where ∇ denotes the gradient operator.

As a development, for the fractional second-grade fluid when considering the memory characteristics [21], the stress tensor τ has the following expression

$$\tau = \mu A_1 + \alpha_1 A_2 + \alpha_2 A_1^2, \tag{2}$$

where μ refers to the dynamic viscosity, α_1 and α_2 denote the material moduli, A_1 and A_2 are the kinematic tensors with the expression as

$$A_1 = \nabla V + (\nabla V)^T \text{ and } A_2 = D_t^\alpha A_1 + A_1 \nabla V + (\nabla V)^T A_1, \tag{3}$$

where D_t^α denotes the Riemann–Liouville's fractional operator of order α $(0 < a < 1)$ [43], the definition for a function $f(t)$ defined on $[t_1, t_2]$ is given as

$$D_t^\alpha f(t) = \frac{d}{dt}\left(\frac{1}{\Gamma(1-\alpha)}\int_{t_1}^{t} \frac{f(\xi)}{(t-\xi)^\alpha}d\xi\right). \tag{4}$$

For considering the Clausius–Duhem inequality and assuming that the minimum at equilibrium for the Helmholtz free energy is [44,45], the material constants satisfy the following restrictions

$$\mu \geq 0, \ \alpha_1 \geq 0 \text{ and } \alpha_1 + \alpha_2 = 0. \tag{5}$$

Applying the periodic pressure gradient into the z-direction, the motion of second-grade fluid in the direction is parallel to the axial coordinate with an oscillating form. The velocity field is assumed as

$$V = [0, 0, w(x, y, t)]^T, \tag{6}$$

where $w(x, y, t)$ refers to the velocity in the z-direction. For this consideration, it is simple to find that the continuity Equation (1) automatically satisfies consideration of the velocity field (6).

Considering the effect of an electromagnetic field, the motion equation for describing the second-grade fluid is denoted as follows

$$\rho D_t V = -\nabla p + \nabla \cdot \tau - \sigma_0 B_0^2 V, \tag{7}$$

where V corresponds to the velocity vector, ρ refers to the fluid density, p denotes the hydrostatic pressure, the operator D_t refers to the material derivative, σ_0 refers to electrical conductivity and B_0 is the magnetic field.

Combining the expansion of Equation (2) (see the Appendix A) with Equation (7), the fractional governing equation can be derived as

$$\frac{\partial w}{\partial t} = \nu(1 + \lambda D_t^\alpha)\left(\frac{\partial^2 w}{\partial x^2} + \frac{\partial^2 w}{\partial y^2}\right) - Mw - \frac{1}{\rho}\frac{\partial p}{\partial z}, \tag{8}$$

where $\nu = \frac{\mu}{\rho}$ denotes the kinematic viscosity, $\lambda = \frac{\alpha_1}{\mu}$ refers to the retardation time, $M = \frac{\sigma_0 B_0^2}{\rho}$ corresponds to the magnetic parameter.

The initial conditions are

$$w(x, y, 0) = 0, \tag{9}$$

and the boundary conditions regardless of slip are given as

$$w(\pm a, y, t) = w(x, \pm b, t) = 0. \tag{10}$$

The initial boundary conditions of (9) and (10) are the Dirichlet type based on the physical backgrounds considering a laminar flow in a straight duct with infinite length and rectangular cross-section. When the boundary conditions change to Neumann, Robin or some other kind of initial boundary conditions, the physical meaning of this paper changes. However, the treatment process of the fractional governing equation with the difference method and the fast algorithm is also applicable. The only difference is the boundary discretization is slightly different.

Theorem 1. *[43] Assume a positive α satisfies $0 \leq n - 1 < \alpha < n$. Suppose the function $f(t)$ in region $[t_1, t_2]$ has $n - 1$ continuous bounded derivative for every $t_2 > t_1$, then*

$$D_t^\alpha f(t) = {}^C D_t^\alpha f(t) + \sum_{j=1}^{n-1} \frac{f^{(j)}(t_1)(t - t_1)^{j-\alpha}}{\Gamma(1 + j - \alpha)}, \ t_1 \leq t \leq t_2, \tag{11}$$

where ${}^C D_t^\alpha f(t)$ refers to the Caputo's fractional derivative [43].

Through Theorem 1, we have $D_t^\alpha f(t) = {}^C D_t^\alpha f(t)$ with the condition that second-grade fluid flowing along a straight rectangular duct is subjected to the zero initial condition. In the following discussions, we are able to substitute the Riemann–Liouville derivative with Caputo's derivative.

3. Analytical Solution

In this part, we try to obtain the analytical solution of (8)–(10). Firstly, we consider the equation:

$$\frac{\partial u}{\partial t} = \nu \left(\frac{\partial^2 u}{\partial x^2} + \frac{\partial^2 u}{\partial y^2} \right) - Mu, \tag{12}$$

$$u(\pm 1, y, t, \tau) = u(x, \pm 1, t, \tau) = 0. \tag{13}$$

To simplify the calculation, we introduce $u(x, y, t, \tau) = h(x + 1, y + 1, t, \tau)$, after which it becomes:

$$\frac{\partial h}{\partial t} = \nu \left(\frac{\partial^2 h}{\partial x^2} + \frac{\partial^2 h}{\partial y^2} \right) - Mh, \tag{14}$$

$$h(0, y, t, \tau) = h(x, 0, t, \tau) = h(2, y, t, \tau) = h(x, 2, t, \tau) = 0 \tag{15}$$

The solution of (14)–(15) is obtained by separation of variables. Defining $h(x, y, t, \tau) = T(t, \tau)\Phi(x, y)$ and the operator $\Delta = \frac{\partial^2}{\partial x^2} + \frac{\partial^2}{\partial y^2}$, yields:

$$\Phi \frac{\partial T}{\partial t} = \nu T \Delta \Phi - MT\Phi, \tag{16}$$

$$\Phi(0, y) = \Phi(x, 0) = \Phi(2, y) = \Phi(x, 2) = 0 \tag{17}$$

Denote

$$\Delta \Phi = \eta \cdot \Phi. \tag{18}$$

It can be deduced immediately that

$$\frac{\partial T}{\partial t} = (\nu \eta - M) T \tag{19}$$

Equation (18) is a Helmholtz equation and the solution with the boundary conditions (17) can be obtained: $\Phi_{n,m} = \sin\left(\frac{n\pi}{2}x\right)\sin\left(\frac{m\pi}{2}y\right)$, where $n, m \in \mathbb{N}$. It can then be deduced that η can only be discrete values with the value $\eta = -\frac{n^2+m^2}{4}\pi^2$. It is simple to determine the solution to Equation (19) as $T = B(\tau)e^{(\nu\eta-M)t}$, where $B(\tau)$ is an arbitrary function. The solution of $h(x, y, t, \tau)$ has the following form

$$h(x, y, t, \tau) = \sum_{n=1}^{+\infty} \sum_{m=1}^{+\infty} B_{n,m}(\tau) e^{-(\nu\pi^2 \frac{n^2+m^2}{4} + M)t} \sin\left(\frac{n\pi}{2}x\right) \sin\left(\frac{m\pi}{2}y\right), \tag{20}$$

and then

$$u(x, y, t, \tau) = \sum_{n=1}^{+\infty} \sum_{m=1}^{+\infty} B_{n,m}(\tau) e^{-(\nu\pi^2 \frac{n^2+m^2}{4} + M)t} \sin\left(\frac{n\pi}{2}(x+1)\right) \sin\left(\frac{m\pi}{2}(y+1)\right) \tag{21}$$

Denote $\frac{1}{\rho}\frac{\partial p}{\partial z} = g(t)$. Equation (8) can be expressed as:

$$\frac{\partial w}{\partial t} = \nu(1 + \lambda D_t^\alpha)\left(\frac{\partial^2 w}{\partial x^2} + \frac{\partial^2 w}{\partial y^2}\right) - Mw - g(t). \tag{22}$$

Suppose there is a function $u(x, y, t, \tau)$ satisfying $w(x, y, t) = \int_0^t u(x, y, t, \tau)d\tau$. Substituting this expression into (21), yields

$$\begin{aligned} u(x, y, t, t) + \int_0^t \frac{\partial u(x,y,t,\tau)}{\partial t}d\tau &= \int_0^t (\nu\Delta u(x, y, t, \tau) - Mu(x, y, t, \tau))d\tau \\ &+ \frac{\nu\lambda}{\Gamma(1-\alpha)}\frac{d}{dt}\int_0^t (t-\xi)^{-\alpha}\int_0^\xi \Delta u(x, y, \xi, \tau)d\tau d\xi - g(t). \end{aligned} \tag{23}$$

From Equation (12), Equation (23) can be reduced as:

$$\frac{\nu\lambda}{\Gamma(1-\alpha)}\frac{d}{dt}\int_0^t (t-\xi)^{-\alpha}\int_0^\xi \Delta u(x,y,\xi,\tau)d\tau d\xi - u(x,y,t,t) = g(t). \qquad (24)$$

Substituting the solution (21) into Equation (24), yields

$$\left[-\frac{\nu\lambda}{\Gamma(1-\alpha)}\sum_{n=1}^{+\infty}\sum_{m=1}^{+\infty}\left(\frac{n^2+m^2}{4}\pi^2\right)\frac{d}{dt}\int_0^t(t-\xi)^{-\alpha}\int_0^\xi B_{n,m}(\tau)d\tau e^{-(\nu\pi^2\frac{n^2+m^2}{4}+M)\xi}d\xi\right.$$
$$\left.-\sum_{n=1}^{+\infty}\sum_{m=1}^{+\infty}B_{n,m}(t)e^{-(\nu\pi^2\frac{n^2+m^2}{4}+M)t}\right]\cdot\sin\left(\frac{n\pi}{2}(x+1)\right)\sin\left(\frac{m\pi}{2}(y+1)\right)=g(t). \qquad (25)$$

Perform the inner product with $\sin\left(\frac{n_0\pi}{2}(x+1)\right)\sin\left(\frac{m_0\pi}{2}(y+1)\right)$ on both sides of Equation (25) and integral interval chosen as $[-1,1]\times[-1,1]$. Then for the left side of the Equation (25), we have:

$$\sum_{n=1}^{+\infty}\sum_{m=1}^{+\infty}C_{n,m}(t)\int_{-1}^1\int_{-1}^1\sin\left(\frac{n\pi}{2}(x+1)\right)\sin\left(\frac{m\pi}{2}(y+1)\right)\sin\left(\frac{n_0\pi}{2}(x+1)\right)\sin\left(\frac{m_0\pi}{2}(y+1)\right)dxdy$$
$$=\sum_{n=1}^{+\infty}\sum_{m=1}^{+\infty}\frac{C_{n,m}(t)}{4}\int_{-1}^1\left[\cos\left(\frac{(n-n_0)\pi}{2}(x+1)\right)-\cos\left(\frac{(n+n_0)\pi}{2}(x+1)\right)\right]dx$$
$$\cdot\int_{-1}^1\left[\cos\left(\frac{(m-m_0)\pi}{2}(y+1)\right)-\cos\left(\frac{(m+m_0)\pi}{2}(y+1)\right)\right]dy$$
$$=C_{n_0,m_0}(t) \qquad (26)$$

where

$$C_{n,m}(t)=-\frac{\nu\lambda\pi^2(n^2+m^2)}{4\Gamma(1-\alpha)}\frac{d}{dt}\int_0^t(t-\xi)^{-\alpha}\int_0^\xi B_{n,m}(\tau)d\tau e^{-(\nu\pi^2\frac{n^2+m^2}{4}+M)\xi}d\xi - B_{n,m}(t)e^{-(\nu\pi^2\frac{n^2+m^2}{4}+M)t}$$

For the right-hand component of Equation (25), the integral is zero when n_0 and m_0 are even. Set $n_0=2k_1-1$, $m_0=2k_2-1$, where k_1 and k_2 are positive integers. Then we have the following integral formula:

$$\int_{-1}^1\int_{-1}^1\sin\left(\frac{(2k_1-1)\pi}{2}(x+1)\right)\sin\left(\frac{(2k_2-1)\pi}{2}(y+1)\right)dxdy = \frac{16}{(2k_1-1)(2k_2-1)\pi^2}. \qquad (27)$$

By a combination of Equations (26) and (27), the following equation can be obtained:

$$\frac{C_{n,m}^{(1)}}{\Gamma(1-\alpha)}\frac{d}{dt}\int_0^t(t-\xi)^{-\alpha}\int_0^\xi B_{n,m}(\tau)d\tau e^{-C_{n,m}^{(2)}\xi}d\xi - B_{n,m}(t)e^{-C_{n,m}^{(2)}t} = C_{n,m}^{(3)}g(t), \qquad (28)$$

where $n=2k_1-1$, $m=2k_2-1$, $C_{n,m}^{(1)}=-\left(\frac{n^2+m^2}{4}\pi^2\right)\nu\lambda$, $C_{n,m}^{(2)}=\nu\pi^2\frac{n^2+m^2}{4}+M$ and $C_{n,m}^{(3)}=\frac{16}{nm\pi^2}$.

Denote $\xi=t-\gamma$, Equation (28) can be rewritten as:

$$\frac{C_{n,m}^{(1)}}{\Gamma(1-\alpha)}\left(\int_0^t\gamma^{-\alpha}B_{n,m}(t-\gamma)e^{C_{n,m}^{(2)}(\gamma-t)}d\gamma - C_{n,m}^{(2)}\int_0^t\gamma^{-\alpha}\int_0^{t-\gamma}B_{n,m}(\tau)d\tau e^{C_{n,m}^{(2)}(\gamma-t)}d\gamma\right)$$
$$-B_{n,m}(t)e^{-C_{n,m}^{(2)}t}=C_{n,m}^{(3)}g(t). \qquad (29)$$

Denote $t=0$, we have the relationship:

$$B_{n,m}(0)=-C_{n,m}^{(3)}g(0). \qquad (30)$$

Multiplying the left and right sides of (29) by $e^{C_{n,m}^{(2)}t}$ and taking the derivative of t, yields:

$$\frac{C_{n,m}^{(1)}}{\Gamma(1-\alpha)}\left(t^{-\alpha}B_{n,m}(0)e^{C_{n,m}^{(2)}t} + \int_0^t \gamma^{-\alpha}B_{n,m}{}'(t-\gamma)e^{C_{n,m}^{(2)}\gamma}d\gamma - C_{n,m}^{(2)}\int_0^t \gamma^{-\alpha}B_{n,m}(t-\gamma)e^{C_{n,m}^{(2)}\gamma}d\gamma\right)$$
$$- \frac{dB_{n,m}(t)}{dt} = e^{C_{n,m}^{(2)}t}C_{n,m}^{(3)}\left(C_{n,m}^{(2)}g(t) + g'(t)\right). \tag{31}$$

Resort to variable $\gamma = t - \xi$ and multiply both sides of Equation (31) by $e^{-C_{n,m}^{(2)}t}$, we have:

$$\frac{C_{n,m}^{(1)}}{\Gamma(1-\alpha)}\int_0^t (t-\xi)^{-\alpha}\frac{dB_{n,m}(\xi)e^{-C_{n,m}^{(2)}\xi}}{d\xi}d\xi - \frac{dB_{n,m}(t)e^{-C_{n,m}^{(2)}t}}{dt} - C_{n,m}^{(2)}B_{n,m}(t)e^{-C_{n,m}^{(2)}t}$$
$$= C_{n,m}^{(3)}\left(C_{n,m}^{(2)}g(t) + g'(t)\right) - \frac{C_{n,m}^{(1)}}{\Gamma(1-\alpha)}t^{-\alpha}B_{n,m}(0). \tag{32}$$

Denoting $A_{n,m}(t) = B_{n,m}(t)e^{-C_{n,m}^{(2)}t}$ and according to (30), we have

$$C_{n,m}^{(1)}\frac{d^{\alpha+1}A_{n,m}}{dt^{\alpha+1}} - \frac{dA_{n,m}}{dt} - C_{n,m}^{(2)}A_{n,m} = C_{n,m}^{(3)}\left(C_{n,m}^{(2)}g(t) + g'(t)\right) - \frac{C_{n,m}^{(1)}A_{n,m}(0)}{\Gamma(1-\alpha)}t^{-\alpha}, \tag{33}$$

where $n = 2k_1 - 1$, $m = 2k_2 - 1$ and $A_{n,m}(0) = -C_{n,m}^{(3)}g(0)$. The analytical solution can be obtained by referring to [46].

Then the solution to Equation (20) can be obtained as:

$$w(x,y,t) = \sum_{\substack{n = 1 \\ n = 2k_1 - 1}}^{+\infty} \sum_{\substack{m = 1 \\ m = 2k_2 - 1}}^{+\infty} \int_0^t B_{n,m}(\tau)d\tau \cdot e^{-(v\pi^2\frac{n^2+m^2}{4}+M)t}\sin\left(\frac{n\pi}{2}(x+1)\right)\sin\left(\frac{m\pi}{2}(y+1)\right), \tag{34}$$

where $B_{n,m}(t) = e^{C_{n,m}^{(2)}t}A_{n,m}(t)$ and $A_{n,m}(t)$ refers to the solution of (33).

4. Numerical Discretization Method

Numerical Scheme

Firstly, we divide the spatial region $[-a,a] \times [-b,b]$ with the uniform mesh points $x_i = -a + ih_x$, $i = 0, 1, \cdots, M_x$, $y_j = -b + jh_y$, $j = 0, 1, \cdots, M_y$, in which $h_x = 2a/M_x$, $h_y = 2b/M_y$. For the time region $[0, T]$, we take $t_n = n\tau$ with time step $\tau = T/N$ for $n = 0, 1, \cdots N$. Define $\Omega_h \equiv \left\{(x_i, y_j)\big| 0 \le i \le M_x, 0 \le j \le M_y\right\}$ and $\Omega_\tau \equiv \{t_n | 0 \le n \le N\}$.

For a net function $w = \left\{w_{i,j}^n \big| 0 \le i \le M_x, 0 \le j \le M_y, 0 \le n \le N\right\}$ defined on an interval $\Omega_h \times \Omega_\tau$, denote the following symbols for simplicity:

$$\nabla_t w_{i,j}^n = \frac{w_{i,j}^n - w_{i,j}^{n-1}}{\tau}, \quad \delta_x w_{i,j}^n = \frac{w_{i,j}^n - w_{i-1,j}^n}{h_x}, \quad \delta_y w_{i,j}^n = \frac{w_{i,j}^n - w_{i,j-1}^n}{h_y},$$

$$\delta_x^2 w_{i,j}^n = \frac{w_{i+1,j}^n - 2w_{i,j}^n + w_{i-1,j}^n}{h_x^2}, \quad \delta_y^2 w_{i,j}^n = \frac{w_{i,j+1}^n - 2w_{i,j}^n + w_{i,j-1}^n}{h_x^2}$$

Furthermore, the exact solution is defined as $W_{i,j}^n = w(x_i, y_j, t_n)$ for simplicity. Applying the L1-scheme [37] for discretizing the fractional derivative, at the mesh points (x_i, y_j, t_n), we have:

$$\frac{\partial^\alpha W_{i,j}^n}{\partial t^\alpha} = \frac{\tau^{-\alpha}}{\Gamma(2-\alpha)}\left(c_0 W_{i,j}^n - \sum_{k=1}^{n-1}(c_{n-k-1} - c_{n-k})W_{i,j}^k - c_{n-1}W_{i,j}^0\right) + (R_1)_{i,j}^n \tag{35}$$

where $c_k = (k+1)^{1-\alpha} - k^{1-\alpha}$ and $\left|(R_1)_{i,j}^n\right| \le C\tau^{2-\alpha}$.

At the mesh points (x_i, y_j, t_n), the backward difference method is applied to discretize the time derivative of order one

$$\frac{\partial W_{i,j}^n}{\partial t} = \nabla_t W_{i,j}^n + O(\tau) \tag{36}$$

Use of the central difference scheme yields the discretization schemes for the second order space derivatives

$$\frac{\partial^2 W_{i,j}^n}{\partial x^2} = \delta_x^2 W_{i,j}^n + O\left(h_x^2\right) \text{ and } \frac{\partial^2 W_{i,j}^n}{\partial y^2} = \delta_y^2 W_{i,j}^n + O\left(h_y^2\right) \tag{37}$$

Combining (35) and (37), we have the difference schemes for the mixed derivatives of time and space:

$$\frac{\partial^\alpha}{\partial t^\alpha} \frac{\partial^2}{\partial x^2} W_{i,j}^n = \frac{\tau^{-\alpha}}{\Gamma(2-\alpha)} \left(c_0 \delta_x^2 W_{i,j}^n - \sum_{k=1}^{n-1} (c_{n-k-1} - c_{n-k}) \delta_x^2 W_{i,j}^k - c_{n-1} \delta_x^2 W_{i,j}^0 \right) + (R_2)_{i,j}^n, \tag{38}$$

$$\frac{\partial^\alpha}{\partial t^\alpha} \frac{\partial^2}{\partial y^2} W_{i,j}^n = \frac{\tau^{-\alpha}}{\Gamma(2-\alpha)} \left(c_0 \delta_y^2 W_{i,j}^n - \sum_{k=1}^{n-1} (c_{n-k-1} - c_{n-k}) \delta_y^2 W_{i,j}^k - c_{n-1} \delta_y^2 W_{i,j}^0 \right) + (R_3)_{i,j}^n, \tag{39}$$

where $\left| (R_2)_{i,j}^n \right| \leq C\left(\tau^{2-\alpha} + h_x^2\right)$ and $\left| (R_3)_{i,j}^n \right| \leq C\left(\tau^{2-\alpha} + h_y^2\right)$.

Denote the discretization scheme for $-\frac{1}{\rho} \frac{\partial p}{\partial z}$ at the points (x_i, y_j, t_n) as $g_{i,j}^n$. Through the difference schemes (35)–(39), we have the final discretization scheme for the governing Equation (8)

$$
\begin{aligned}
&\nabla_t W_{i,j}^n + M W_{i,j}^n - \nu \delta_x^2 W_{i,j}^n - \nu \delta_y^2 W_{i,j}^n \\
&= \nu\lambda \frac{\tau^{-\alpha}}{\Gamma(2-\alpha)} \left(c_0 \delta_x^2 W_{i,j}^n - \sum_{k=1}^{n-1} (c_{n-k-1} - c_{n-k}) \delta_x^2 W_{i,j}^k - c_{n-1} \delta_x^2 W_{i,j}^0 \right) \\
&+ \nu\lambda \frac{\tau^{-\alpha}}{\Gamma(2-\alpha)} \left(c_0 \delta_y^2 W_{i,j}^n - \sum_{k=1}^{n-1} (c_{n-k-1} - c_{n-k}) \delta_y^2 W_{i,j}^k - c_{n-1} \delta_y^2 W_{i,j}^0 \right) + g_{i,j}^n + R_{i,j}^n,
\end{aligned}
\tag{40}
$$

where $\left| R_{i,j}^n \right| \leq C\left(\tau + h_x^2 + h_y^2\right)$.

Substituting $W_{i,j}^n$ with $w_{i,j}^n$, we have the numerical difference scheme of Equation (8)

$$
\begin{aligned}
&\nabla_t w_{i,j}^n + M w_{i,j}^n - \nu \delta_x^2 w_{i,j}^n - \nu \delta_y^2 w_{i,j}^n \\
&= \nu\lambda \frac{\tau^{-\alpha}}{\Gamma(2-\alpha)} \left(c_0 \delta_x^2 w_{i,j}^n - \sum_{k=1}^{n-1} (c_{n-k-1} - c_{n-k}) \delta_x^2 w_{i,j}^k - c_{n-1} \delta_x^2 w_{i,j}^0 \right) \\
&+ \nu\lambda \frac{\tau^{-\alpha}}{\Gamma(2-\alpha)} \left(c_0 \delta_y^2 w_{i,j}^n - \sum_{k=1}^{n-1} (c_{n-k-1} - c_{n-k}) \delta_y^2 w_{i,j}^k - c_{n-1} \delta_y^2 w_{i,j}^0 \right) + g_{i,j}^n.
\end{aligned}
\tag{41}
$$

By merging the terms at the same time layer, making the left side the n-th time layer, and the right side the time layer with the order less than n, Equation (41) can be rewritten in another form:

$$
\begin{aligned}
&\left(\frac{1}{\tau} + M\right) w_{i,j}^n - \frac{\nu}{h_x^2}(r_1 + 1)\left(w_{i+1,j}^n - 2w_{i,j}^n + w_{i-1,j}^n \right) - \frac{\nu}{h_y^2}(r_1 + 1)\left(w_{i,j+1}^n - 2w_{i,j}^n + w_{i,j-1}^n \right) \\
&= \frac{1}{\tau} w_{i,j}^{n-1} - \nu r_1 \left[\sum_{k=1}^{n-1} (c_{n-k-1} - c_{n-k}) \left(\delta_x^2 w_{i,j}^k + \delta_y^2 w_{i,j}^k \right) + c_{n-1} \left(\delta_x^2 w_{i,j}^0 + \delta_y^2 w_{i,j}^0 \right) \right] + g_{i,j}^n,
\end{aligned}
\tag{42}
$$

where $r_1 = \frac{\lambda \tau^{-\alpha}}{\Gamma(2-\alpha)}$ and $g_{i,j}^n = -\frac{1}{\rho} \frac{\partial p(x_i, y_j, t_n)}{\partial z}$.

In what follows, the symbol E denotes the unit matrix which may be with a different order in various sections. Considering the zero-boundary conditions, the discretization scheme (42) can be rewritten in a matrix form:

$$\left(\frac{1}{\tau} + M\right)Ew^n - \frac{\nu(r_1+1)}{h_x^2}E \otimes K_1 w^n - \frac{\nu(r_1+1)}{h_y^2}K_2 \otimes Ew^n$$
$$= \frac{1}{\tau}Ew^{n-1} - \nu r_1 \left[\sum_{k=1}^{n-1}(c_{n-k-1} - c_{n-k})(E \otimes K_1 + K_2 \otimes E)w^k + c_{n-1}(E \otimes K_1 + K_2 \otimes E)w^0\right] + g^n,$$

where the symbol $\otimes$ denotes the Kronecker product [47],

$$K_1 = \begin{pmatrix} -2 & 1 & & & \\ 1 & -2 & 1 & & \\ & \ddots & \ddots & \ddots & \\ & & 1 & -2 & 1 \end{pmatrix}_{(M_x-1)\times(M_x-1)}, K_2 = \begin{pmatrix} -2 & 1 & & & \\ 1 & -2 & 1 & & \\ & \ddots & \ddots & \ddots & \\ & & 1 & -2 & 1 \end{pmatrix}_{(M_y-1)\times(M_y-1)},$$

$$w^n = \left(w_{1,1}^n, w_{2,1}^n, \ldots, w_{M_x-1,1}^n, w_{1,2}^n, w_{2,2}^n, \ldots, w_{M_x-1,2}^n, \ldots, w_{1,M_y-1}^n, w_{2,M_y-1}^n, \ldots, w_{M_x-1,M_y-1}^n\right)^T,$$

$$g^n = \left(g_{1,1}^n, g_{2,1}^n, \ldots, g_{M_x-1,1}^n, g_{1,2}^n, g_{2,2}^n, \ldots, g_{M_x-1,2}^n, \ldots, g_{1,M_y-1}^n, g_{2,M_y-1}^n, \ldots, g_{M_x-1,M_y-1}^n\right)^T.$$

The initial condition can be discretized as $w_{i,j}^0 = 0$ and the boundary conditions are discretized as $w_{0,j}^n = w_{M_x,j}^n = w_{i,0}^n = w_{i,M_y}^n = 0$. The above numerical method can be applied to widespread situations, for example, the dynamics in porous media for solving Richards' equation [48]. For this equation, the treating method mentioned above can be similarly applied.

Besides the velocity distribution, the shear force is another important quantity to analyze. We consider the shear force τ_{xz} for xz-direction at the wall surface ($x = 0$), and the difference scheme is given as:

$$\tau_{xz} = (\mu + \alpha_1 D_t^\alpha)\frac{\partial w}{\partial x}\bigg|_{x=0}$$
$$\approx \left[\mu + \frac{\alpha_1 \tau^{-\alpha}}{\Gamma(2-\alpha)}\right]\frac{w_{1,j}^n - w_{0,j}^n}{h_x} - \frac{\alpha_1 \tau^{-\alpha}}{\Gamma(2-\alpha)}\sum_{k=1}^{n-1}(c_{n-k-1} - c_{n-k})\frac{w_{1,j}^k - w_{0,j}^k}{h_x} - \frac{\alpha_1 \tau^{-\alpha}c_{n-1}}{\Gamma(2-\alpha)}\frac{w_{1,j}^0 - w_{0,j}^0}{h_x}.$$

Due to the symmetry of the velocity in the x- and y-directions, we deduce the shear force along the yz-direction at the wall surface $y = 0$ to be the same as the xz-direction.

5. Feasibility Analysis

Denote $V_h = \{v|v\}$ is a net function on $\Omega_h \times \Omega_\tau$, $v_{i,j}^n = 0$ when $i = 0$ and M_x or $j = 0$ and M_y. For w^n, $v^n \in V_h$, we denote the discrete inner products and norms:

$$(w^n, v^n) = h_x h_y \sum_{i=1}^{M_x-1}\sum_{i=1}^{M_y-1} w_{i,j}^n v_{i,j}^n \text{ and } \| w^n \|^2 = (w^n, w^n). \tag{43}$$

Lemma 1. *[49] The matrix* $\mathbf{A} \otimes \mathbf{B}$ *is symmetric positive definite with the condition that both* $\mathbf{A} \in \mathbb{R}^{n \times n}$ *and* $\mathbf{B} \in \mathbb{R}^{n \times n}$ *satisfy symmetric positive definite. For* $\forall 0 \neq \mathbf{v} \in \mathbb{R}^{n^2}$, *it holds that:*

$$\mathbf{v}^T(\mathbf{A} \otimes \mathbf{B})\mathbf{v} > 0. \tag{44}$$

Lemma 2. *[50] For all* $\mathbf{A}$ *and* $\mathbf{B}$, $(\mathbf{A} \otimes \mathbf{B})^T = \mathbf{A}^T \otimes \mathbf{B}^T$.

Lemma 3. *For* $w, v \in \Omega_h \times \Omega_\tau$, *it is straightforward to check that* $\left(\delta_x^2 w^k, v^k \right) = - \left(\delta_x w^k, \delta_x v^k \right)$ *with the zero-boundary conditions by applying integration by parts.*

Lemma 4. *[37] For the symbols* c_j *in (35), define the vector* $S = [S_1, S_2, \ldots, S_N]^T$ *and constant* P, *it holds that:*

$$\frac{\tau^{-\alpha}}{\Gamma(2-\alpha)} \sum_{k=1}^{N} \left[c_0 S_k - \sum_{j=1}^{k-1} \left(c_{k-j-1} - c_{k-j} \right) S_j - c_{k-1} P \right] S_k \geq \frac{T^{-\alpha}}{2\Gamma(1-\alpha)} \sum_{k=1}^{N} S_k^2 - \frac{T^{1-\alpha}}{2\tau\Gamma(2-\alpha)} P^2$$

5.1. Solvability

Theorem 2. *Denote* $w_{i,j}^n$ *as the numerical solution of Equations (8)–(10) for* $i = 0, 1, \cdots, M_x$, $j = 0, 1, \cdots, M_y$ *and* $n = 0, 1, \cdots N$, *then (42) is uniquely solvable.*

Proof. Denote the coefficient matrix $\mathbf{G} = \left(\frac{1}{\tau} + M \right) E - \frac{\nu(r_1+1)}{h_x^2} E \otimes K_1 - \frac{\nu(r_1+1)}{h_y^2} K_2 \otimes E$. Firstly, using Lemma 3, we have:

$$\mathbf{G}^T = \left(\frac{1}{\tau} + M \right) E^T - \frac{\nu(r_1+1)}{h_x^2} E^T \otimes K_1^T - \frac{\nu(r_1+1)}{h_y^2} K_2^T \otimes E^T = \mathbf{G}$$

Furthermore, the matrix $\mathbf{G}$ can simply be verified as strictly diagonally dominant. Then, the matrix $\mathbf{G}$ is positive definite. Therefore, the numerical difference scheme has a unique solution. $\square$

5.2. Stability

Theorem 3. *The scheme (41) possesses unconditional stability, which satisfies:*

$$\|w_{i,j}^N\|^2 \leq \frac{T}{2M} \max_{1 \leq n \leq N} \|g_{i,j}^n\|^2$$

Proof. Multiplying both sides of Equation (41) by $\tau h_x h_y w_{i,j}^n$, and summing i, j, n from 1 to $M_x - 1$, 1 to $M_y - 1$, 1 to N, respectively, we derive the following equation:

$$\tau h_x h_y \sum_{i=1}^{M_x-1} \sum_{i=1}^{M_y-1} \sum_{n=1}^{N} w_{i,j}^n \nabla_t w_{i,j}^n + M\tau h_x h_y \sum_{i=1}^{M_x-1} \sum_{i=1}^{M_y-1} \sum_{n=1}^{N} w_{i,j}^n w_{i,j}^n - \nu\tau h_x h_y \sum_{i=1}^{M_x-1} \sum_{i=1}^{M_y-1} \sum_{n=1}^{N} w_{i,j}^n \left(\delta_x^2 w_{i,j}^n - \delta_y^2 w_{i,j}^n \right)$$

$$- \frac{\nu\lambda\tau^{-\alpha}}{\Gamma(2-\alpha)} \tau h_x h_y \sum_{i=1}^{M_x-1} \sum_{i=1}^{M_y-1} \sum_{n=1}^{N} \left(c_0 \delta_x^2 w_{i,j}^n - \sum_{k=1}^{n-1} (c_{n-k-1} - c_{n-k}) \delta_x^2 w_{i,j}^k - c_{n-1} \delta_x^2 w_{i,j}^0 \right) w_{i,j}^n$$

$$- \frac{\nu\lambda\tau^{-\alpha}}{\Gamma(2-\alpha)} \tau h_x h_y \sum_{i=1}^{M_x-1} \sum_{i=1}^{M_y-1} \sum_{n=1}^{N} \left(c_0 \delta_y^2 w_{i,j}^n - \sum_{k=1}^{n-1} (c_{n-k-1} - c_{n-k}) \delta_y^2 w_{i,j}^k - c_{n-1} \delta_y^2 w_{i,j}^0 \right) w_{i,j}^n$$

$$= \tau h_x h_y \sum_{i=1}^{M_x-1} \sum_{i=1}^{M_y-1} \sum_{n=1}^{N} w_{i,j}^n g_{i,j}^n.$$

By applying the inequation $a(a - b) \geq \frac{1}{2}(a^2 - b^2)$ and considering the zero initial condition, the first term satisfies:

$$\tau h_x h_y \sum_{i=1}^{M_x-1} \sum_{i=1}^{M_y-1} \sum_{n=1}^{N} w_{i,j}^n \nabla_t w_{i,j}^n \geq \frac{1}{2} h_x h_y \sum_{i=1}^{M_x-1} \sum_{i=1}^{M_y-1} \sum_{n=1}^{N} \left[\left(w_{i,j}^n \right)^2 - \left(w_{i,j}^{n-1} \right)^2 \right]$$

$$= \frac{1}{2} h_x h_y \sum_{i=1}^{M_x-1} \sum_{i=1}^{M_y-1} \left[\left(w_{i,j}^N \right)^2 - \left(w_{i,j}^0 \right)^2 \right] = \frac{1}{2} \left(\|w^N\|^2 - \|w^0\|^2 \right) = \frac{1}{2} \|w^N\|^2.$$

Considering the relationship between the norm and inner product, the second term yields

$$M\tau h_x h_y \sum_{i=1}^{M_x-1} \sum_{i=1}^{M_y-1} \sum_{n=1}^{N} w_{i,j}^n w_{i,j}^n = M\tau \sum_{n=1}^{N} \left(w_{i,j}^n, w_{i,j}^n \right) = M\tau \sum_{n=1}^{N} \|w^n\|^2$$

By using the Lemma 3, for the third term, we have

$$-\nu\tau h_x h_y \sum_{i=1}^{M_x-1} \sum_{i=1}^{M_y-1} \sum_{n=1}^{N} w_{i,j}^n \left(\delta_x^2 w_{i,j}^n + \delta_y^2 w_{i,j}^n \right)$$

$$= \nu\tau h_x h_y \sum_{i=1}^{M_x-1} \sum_{i=1}^{M_y-1} \sum_{n=1}^{N} \delta_x w_{i,j}^n \delta_x w_{i,j}^n + \nu\tau h_x h_y \sum_{i=1}^{M_x-1} \sum_{i=1}^{M_y-1} \sum_{n=1}^{N} \delta_y w_{i,j}^n \delta_y w_{i,j}^n$$

$$= \nu\tau \sum_{n=1}^{N} \|\delta_x w^n\|^2 + \nu\tau \|\delta_y w^n\|^2 \geq 0$$

By applying Lemma 4, the fourth term satisfies:

$$-\frac{\nu\lambda\tau^{-\alpha}}{\Gamma(2-\alpha)} \tau h_x h_y \sum_{i=1}^{M_x-1} \sum_{i=1}^{M_y-1} \sum_{n=1}^{N} \left(c_0 \delta_x^2 w_{i,j}^n - \sum_{k=1}^{n-1} (c_{n-k-1} - c_{n-k}) \delta_x^2 w_{i,j}^k - c_{n-1} \delta_x^2 w_{i,j}^0 \right) w_{i,j}^n$$

$$= \frac{\nu\lambda\tau^{-\alpha}}{\Gamma(2-\alpha)} \tau h_x h_y \sum_{i=1}^{M_x-1} \sum_{i=1}^{M_y-1} \sum_{n=1}^{N} \left(c_0 \delta_x w_{i,j}^n - \sum_{k=1}^{n-1} (c_{n-k-1} - c_{n-k}) \delta_x w_{i,j}^k - c_{n-1} \delta_x w_{i,j}^0 \right) \delta_x w_{i,j}^n$$

$$\geq \nu\lambda\tau h_x h_y \sum_{i=1}^{M_x-1} \sum_{i=1}^{M_y-1} \left[\frac{T^{-\alpha}}{2\Gamma(1-\alpha)} \sum_{n=1}^{N} \left(\delta_x w_{i,j}^n \right)^2 - \frac{T^{1-\alpha}}{2\tau\Gamma(2-\alpha)} \left(\delta_x w_{i,j}^0 \right)^2 \right]$$

$$= \frac{\nu\lambda\tau T^{-\alpha}}{2\Gamma(1-\alpha)} \sum_{n=1}^{N} \|\delta_x w^n\|^2 - \frac{\nu\lambda T^{1-\alpha}}{2\Gamma(2-\alpha)} \|\delta_x w^0\|^2 \geq 0.$$

Similarly, for the fifth term, it satisfies

$$-\frac{\nu\lambda\tau^{-\alpha}}{\Gamma(2-\alpha)} \tau h_x h_y \sum_{i=1}^{M_x-1} \sum_{i=1}^{M_y-1} \sum_{n=1}^{N} \left(c_0 \delta_y^2 w_{i,j}^n - \sum_{k=1}^{n-1} (c_{n-k-1} - c_{n-k}) \delta_y^2 w_{i,j}^k - c_{n-1} \delta_y^2 w_{i,j}^0 \right) w_{i,j}^n \geq 0.$$

By using the Cauchy–Schwartz inequality, the last term changes as:

$$\tau h_x h_y \sum_{i=1}^{M_x-1} \sum_{i=1}^{M_y-1} \sum_{n=1}^{N} w_{i,j}^n g_{i,j}^n = \tau \sum_{n=1}^{N} \left(w_{i,j}^n, g_{i,j}^n \right) \leq M\tau \sum_{n=1}^{N} \|w^n\|^2 + \frac{\tau}{4M} \sum_{n=1}^{N} \|g^n\|^2.$$

As a conclusion, we deduce:

$$\|w^N\|^2 \leq \frac{\tau}{2M} \sum_{n=1}^{N} \|g^n\|^2 \leq \frac{T}{2M} \max_{1 \leq n \leq N} \|g^n\|^2.$$

□

5.3. Convergence

Define the error $e_{i,j}^n = w_{i,j}^n - w(x_i, y_j, t_n)$. Taking the difference between the Equations (40) and (41), we deduce that the error satisfies:

$$\nabla_t e_{i,j}^n + M e_{i,j}^n - \nu\delta_x^2 e_{i,j}^n - \nu\delta_y^2 e_{i,j}^n$$

$$= \nu\lambda \frac{\tau^{-\alpha}}{\Gamma(2-\alpha)} \left(c_0 \delta_x^2 e_{i,j}^n - \sum_{k=1}^{n-1} (c_{n-k-1} - c_{n-k}) \delta_x^2 e_{i,j}^k - c_{n-1} \delta_x^2 e_{i,j}^0 \right)$$

$$+ \nu\lambda \frac{\tau^{-\alpha}}{\Gamma(2-\alpha)} \left(c_0 \delta_y^2 e_{i,j}^n - \sum_{k=1}^{n-1} (c_{n-k-1} - c_{n-k}) \delta_y^2 e_{i,j}^k - c_{n-1} \delta_y^2 e_{i,j}^0 \right) + O\left(\tau + h_x^2 + h_y^2 \right).$$

$$(45)$$

Theorem 4. *The scheme (41) is convergent with the following form:*

$$\|e^N\|^2 \leq \frac{T}{2M}\left(\tau + h_x^2 + h_y^2\right)^2. \tag{46}$$

Proof. Similar to the proof of the stability, substituting the source term with the error, we have:

$$\|e^N\|^2 \leq \frac{\tau}{2M}\sum_{n=1}^{N}\left(\tau + h_x^2 + h_y^2\right)^2 = \frac{T}{2M}\left(\tau + h_x^2 + h_y^2\right)^2. \tag{47}$$

□

6. Acceleration of the Fractional Derivative

The traditional treating method for the fractional derivative is to use the L1 scheme with an expensive cost of computation and storage due to the non-locality that the fractional derivative contains. The difference scheme at $t = t_n$ contains a summation of all values from zero to the current time and the total cost at every spatial point is $O(N^2)$. To reduce the computational and storage cost, a fast algorithm [38] is applied. Here we summarized the main idea of the fast algorithm.

The definition of Caputo's fractional derivative of order $0 < \alpha < 1$ can be expressed as the summation of two terms, a local part $C_l(t_n)$ and a history part $C_h(t_n)$:

$$\begin{aligned}
{}^{C}D_t^{\alpha}w(t)\big|_{t=t_n} &= \frac{1}{\Gamma(1-\alpha)}\int_0^{t_n}(t_n-s)^{-\alpha}\frac{\partial w(s)}{\partial s}ds \\
&= \frac{1}{\Gamma(1-\alpha)}\int_{t_{n-1}}^{t_n}\frac{1}{(t_n-s)^{\alpha}}\frac{\partial w(s)}{\partial s}ds + \frac{1}{\Gamma(1-\alpha)}\int_0^{t_{n-1}}\frac{1}{(t_n-s)^{\alpha}}\frac{\partial w(s)}{\partial s}ds \\
&:= C_l(t_n) + C_h(t_n).
\end{aligned} \tag{48}$$

For the local portion, we approximate $\frac{\partial w(s)}{\partial s}$ by $\frac{w(t_n)-w(t_{n-1})}{\tau}$, yields

$$C_l(t_n) \approx \frac{w(t_n) - w(t_{n-1})}{\tau\Gamma(1-\alpha)}\int_{t_{n-1}}^{t_n}\frac{ds}{(t_n-s)^{\alpha}} = \frac{w(t_n) - w(t_{n-1})}{\tau^{\alpha}\Gamma(2-\alpha)}. \tag{49}$$

We employ the integration by parts for the history part

$$C_h(t_n) = \frac{1}{\Gamma(1-\alpha)}\left[\frac{w(t_{n-1})}{\tau^{\alpha}} - \frac{w(t_0)}{t_n^{\alpha}} - \alpha\int_0^{t_{n-1}}\frac{w(s)}{(t_n-s)^{\alpha+1}}ds\right]. \tag{50}$$

Treating the kernel $\frac{1}{t^{\alpha+1}}$ in the convolution integral is the key. Referring to [38], for any time interval $[\tau, T]$, the kernel $\frac{1}{t^{\alpha+1}}$ can be approached by an efficient sum-of-exponentials approximation with a prescribed absolute error ε. Specifically speaking, there are real positive numbers w_l and s_l ($l = 1, \cdots, N_{\exp}$) such that

$$\left|\frac{1}{t^{\alpha+1}} - \sum_{l=1}^{N_{\exp}}\omega_l e^{-s_l t}\right| \leq \varepsilon, \text{ for any } t \in [\tau, T], \tag{51}$$

where $N_{\exp}$ is of the order

$$N_{\exp} = \mathcal{O}\left(\log\frac{1}{\varepsilon}\left(\log\log\frac{1}{\varepsilon} + \log\frac{T}{\sigma}\right) + \log\frac{1}{\sigma}\left(\log\log\frac{1}{\varepsilon} + \log\frac{1}{\sigma}\right)\right). \tag{52}$$

Equation (4) is the main idea for the fast algorithm. The sum-of-exponentials approximation for the kernel $\frac{1}{t^{\beta}}$ can also be generalized for the order $0 < \alpha < 2$ [38,51].

We substitute the kernel $\frac{1}{t^{\alpha+1}}$ via the formular (51) to approximate the history portion as:

$$C_h(t_n) \approx \frac{1}{\Gamma(1-\alpha)}\left[\frac{w(t_{n-1})}{\tau^\alpha} - \frac{w(t_0)}{t_n^\alpha} - \alpha\sum_{l=1}^{N_{\exp}}w_l W_{his,l}(t_n)\right], \qquad (53)$$

where $W_{his,l}(t_n) = \int_0^{t_{n-1}} e^{-(t_n-t)s_l}w(t)dt$.

The function $W_{his,l}(t_n)$ is calculated for $n = 1, 2, \cdots, N$ and the following recurrent relationship is derived

$$W_{hist,l}(t_n) = e^{-s_l\tau}W_{hist,l}(t_{n-1}) + \int_{t_{n-2}}^{t_{n-1}} e^{-s_l(t_n-\tau)}w(\tau)d\tau, \ W_{hist,l}(t_0) = 0. \qquad (54)$$

The integral in (54) could be rewritten as:

$$\int_{t_{n-2}}^{t_{n-1}} e^{-s_l(t_n-\tau)}w(\tau)d\tau \approx \frac{e^{-s_l\tau}}{s_l^2\tau}\left[(e^{-s_l\tau}-1+s_l\tau)w^{n-1} + \left(1 - e^{-s_l\tau} - e^{-s_l\tau}s_l\tau\right)w^{n-2}\right]. \qquad (55)$$

To compute $W_{his,i}(t_n)$, as Equation (55) indicates, $W_{his,i}(t_{n-1})$ is already computed and stored and the cost is needed by only O(1) at each step. As (6.4) indicates, the cost to evaluate the fractional derivative is needed $O(N_{\exp})$ at each time step. That is to say, a reduction from O(N) to O($\log N$) or $O\left(\log^2 N\right)$.

As a summation, the fast evolution of the Caputo's fractional derivative at $t = t_n$ is given as:

$$^F D_t^\alpha w(x,y,t_n) = \frac{W^n - W^{n-1}}{\tau^\alpha\Gamma(2-\alpha)} + \frac{1}{\Gamma(1-\alpha)}\left[\frac{W^{n-1}}{\tau^\alpha} - \frac{W^0}{t_n^\alpha} - \alpha\sum_{l=1}^{N_{\exp}}\omega_l W_{hist,l}(t_n)\right] + R_1, \qquad (56)$$

where $|R_1| \le C\left(\tau^{2-\alpha} + \varepsilon\right)$ and the recurrence relation satisfies (6.7) and (6.8).

Combining (56) and (37), we have:

$$\frac{\partial^\alpha}{\partial t^\alpha}\frac{\partial^2}{\partial x^2}w_{i,j}^n = \frac{\delta_x^2 w_{i,j}^n - \delta_x^2 w_{i,j}^{n-1}}{\tau^\alpha\Gamma(2-\alpha)} + \frac{1}{\Gamma(1-\alpha)}\left[\frac{\delta_x^2 w_{i,j}^{n-1}}{\tau^\alpha} - \frac{\delta_x^2 w_{i,j}^0}{t_n^\alpha} - \alpha\sum_{l=1}^{N_{\exp}}\omega_l\delta_x^2 w_{hist,l}(t_n)\right], \qquad (57)$$

$$\frac{\partial^\alpha}{\partial t^\alpha}\frac{\partial^2}{\partial y^2}w_{i,j}^n = \frac{\delta_y^2 w_{i,j}^n - \delta_y^2 w_{i,j}^{n-1}}{\tau^\alpha\Gamma(2-\alpha)} + \frac{1}{\Gamma(1-\alpha)}\left[\frac{\delta_y^2 w_{i,j}^{n-1}}{\tau^\alpha} - \frac{\delta_y^2 w_{i,j}^0}{t_n^\alpha} - \alpha\sum_{l=1}^{N_{\exp}}\omega_l\delta_y^2 w_{hist,l}(t_n)\right], \qquad (58)$$

where $\delta_x^2 w_{hist,l}(t_n) = e^{-s_l\tau}\delta_x^2 w_{hist,l}(t_{n-1}) + \int_{t_{n-2}}^{t_{n-1}} e^{-s_l(t_n-\tau)}\delta_x^2 w(\tau)d\tau$, $\delta_x^2 w_{hist,l}(t_0) = 0$, $\int_{t_{n-2}}^{t_{n-1}} e^{-s_l(t_n-\tau)}\delta_x^2 w(\tau)d\tau \approx \frac{e^{-s_i\tau}}{s_i^2\tau}\left[(e^{-s_i\tau}-1+s_i\tau)\delta_x^2 w^{n-1} + (1-e^{-s_i\tau}-e^{-s_i\tau}s_i\tau)\delta_x^2 w^{n-2}\right]$, $\delta_y^2 w_{hist,l}(t_n) = e^{-s_l\tau}\delta_y^2 w_{hist,l}(t_{n-1}) + \int_{t_{n-2}}^{t_{n-1}} e^{-s_l(t_n-\tau)}\delta_y^2 w(\tau)d\tau$, $\delta_y^2 w_{hist,l}(t_0) = 0$, $\int_{t_{n-2}}^{t_{n-1}} e^{-s_l(t_n-\tau)}\delta_y^2 w(\tau)d\tau \approx \frac{e^{-s_i\tau}}{s_i^2\tau}\left[(e^{-s_i\tau}-1+s_i\tau)\delta_y^2 w^{n-1} + (1-e^{-s_i\tau}-e^{-s_i\tau}s_i\tau)\delta_y^2 w^{n-2}\right]$.

By a combination, we deduce the final difference scheme:

$$\begin{aligned}
&\left(\frac{1}{\tau}+M\right)w_{i,j}^n - \frac{vr_2}{h_x^2}\left(w_{i+1,j}^n - 2w_{i,j}^n + w_{i-1,j}^n\right) - \frac{vr_2}{h_y^2}\left(w_{i,j+1}^n - 2w_{i,j}^n + w_{i,j-1}^n\right) \\
&= \frac{1}{\tau}w_{i,j}^{n-1} + \frac{v\lambda}{\tau^\alpha}\left(\frac{1}{\Gamma(1-\alpha)} - \frac{1}{\Gamma(2-\alpha)}\right)\left(\delta_x^2 w_{i,j}^{n-1} + \delta_y^2 w_{i,j}^{n-1}\right) \\
&\quad - \frac{v\lambda}{\Gamma(1-\alpha)t_n^\alpha}\left(\delta_x^2 w_{i,j}^0 + \delta_y^2 w_{i,j}^0\right) - \frac{v\lambda\alpha}{\Gamma(1-\alpha)}\sum_{l=1}^{N_{\exp}}\omega_l\left[\delta_x^2 w_{hist,l}(t_n) + \delta_y^2 w_{hist,l}(t_n)\right] + g_{i,j}^n,
\end{aligned} \qquad (59)$$

where $r_2 = \frac{\lambda}{\tau^\alpha\Gamma(2-\alpha)} + 1$.

The discretization scheme (59) can be rewritten in a matrix form:

$$\left[\left(\tfrac{1}{\tau}+M\right)E-\tfrac{vr_2}{h_x^2}E\otimes K_1-\tfrac{vr_2}{h_y^2}K_2\otimes E\right]w^n$$
$$=\left[\tfrac{1}{\tau}E+\tfrac{v\lambda}{\tau^\alpha}\left(\tfrac{1}{\Gamma(1-\alpha)}-\tfrac{1}{\Gamma(2-\alpha)}\right)(E\otimes K_1+K_2\otimes E)\right]w^{n-1}+g^n$$
$$-\tfrac{v\lambda}{\Gamma(1-\alpha)t_n^\alpha}(E\otimes K_1+K_2\otimes E)w^0-\tfrac{\alpha v\lambda}{\Gamma(1-\alpha)}\sum_{l=1}^{N_{\exp}}\omega_l\left[\delta_x^2 w_{hist,l}(t_n)+\delta_y^2 w_{hist,l}(t_n)\right]. \tag{60}$$

7. Results and Discussion

Example 1. (*Verification of the discretization scheme*).

The governing equation is solved numerically that the fractional derivative is discretized by the traditional L1 difference method and the fast algorithm. How to verify the correctness of the difference method is the key. As Section 3 indicates, the exact solution is complicated. As a modification, a source term is introduced and the governing equation changes as:

$$\frac{\partial w}{\partial t}=v\left(1+\lambda\frac{D^\alpha}{Dt^\alpha}\right)\left(\frac{\partial^2 w}{\partial x^2}+\frac{\partial^2 w}{\partial y^2}\right)-Mw+f(x,y,t), \tag{61}$$

with the initial distribution and the boundary distributions:

$$w(x,y,0)=0, \tag{62}$$

$$w(\pm 1,y,t)=w(x,\pm 1,t)=0. \tag{63}$$

Define an exact solution for (61)–(63) as: $w(x,y,t)=(x-1)^2(x+1)^2(y-1)^2(y+1)^2 t^2$, the expression of the source term can be deduced:

$$f(x,y,t)=(x-1)^2(x+1)^2(y-1)^2(y+1)^2 t(2+Mt)$$
$$-4vt^2\left(\tfrac{2\lambda}{\Gamma(3-\alpha)}t^{-\alpha}+1\right)\left[(3x^2-1)(y-1)^2(y+1)^2+(3y^2-1)(x-1)^2(x+1)^2\right]. \tag{64}$$

Figure 2 presents the three-dimensional comparison behavior between the numerical and exact expressions. Obviously, the distribution of the numerical solution is basically the same as that of the exact solution, showing a bell-shaped curve that is high in the middle and low at both ends. Tables 1 and 2 show the maximum error with the form $E(h_x,h_y,\tau)=\max\limits_{0\leq i\leq M_x,0\leq j\leq M_y}\left|e_{i,j}^n\right|$, the convergence order for space with $r_s=\log_2\frac{E(h_x,h_y,\tau)}{E(h_x/2,h_y/2,\tau)}$, for time with $r_t=\log_2\frac{E(h_x,h_y,\tau)}{E(h_x,h_y,\tau/2)}$ and the computational time between the classical difference scheme and the fast scheme. The two tables show that the error is very small when verifying the accuracy of the numerical scheme and the accuracy is $\mathrm{O}\left(h_x^2+h_y^2+\tau\right)$, which is consistent with the analysis in the convergence in Theorem 3. Furthermore, the computational time indicates that the superiority of the fast scheme is that it can greatly reduce the calculation time without affecting the total accuracy.
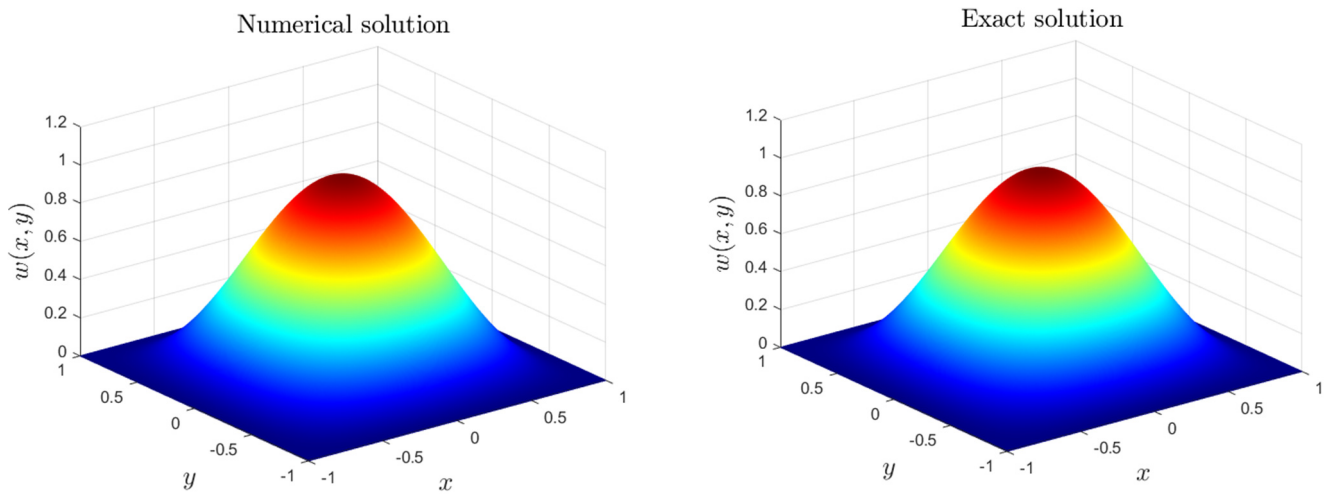
Figure 2. The three-dimensional comparison of velocity distributions for $\alpha = 0.5$, $M = 0.5$ and $\lambda = 0.1$.

Table 1. The error and convergence order for space and the comparison of computational time between the finite difference scheme and the fast scheme when $\alpha = 0.5$, $M = 1$, $\nu = 1$ and $\lambda = 0.1$.

$\tau=1/20000$	Normal L1 Method			Fast Algorithm		
	Error	Order	Time (s)	Error	Order	TIME (s)
$h_x = h_y = 1/2^2$	1.4745×10^{-1}			1.4745×10^{-1}		6.58
$h_x = h_y = 1/2^3$	3.6738×10^{-2}	2.00	317.32	3.6738×10^{-2}	2.00	8.78
$h_x = h_y = 1/2^4$	9.1903×10^{-3}	2.00	2737.48	9.1903×10^{-3}	2.00	14.61
$h_x = h_y = 1/2^5$	2.3032×10^{-3}	2.00	16,424.92	2.3032×10^{-3}	2.00	43.06
$h_x = h_y = 1/2^6$	5.8123×10^{-4}	1.99	59,840.35	5.8123×10^{-4}	1.99	185.47

Table 2. The error and convergence order for time and the comparison of computational time between the finite difference scheme and the fast scheme when $\alpha = 0.5$, $M = 1$, $\nu = 1$ and $\lambda = 0.1$.

$h_x=h_y=1/640$	Normal Scheme			Fast Scheme		
	Error	Order	Time (s)	Error	Order	Time (s)
$\tau = 1/2^2$	3.9307×10^{-2}		2749.74	3.9307×10^{-2}		6.83
$\tau = 1/2^3$	1.9424×10^{-2}	1.02	2851.14	1.9424×10^{-2}	1.02	14.90
$\tau = 1/2^4$	9.5638×10^{-3}	1.02	3057.22	9.5638×10^{-3}	1.02	33.67
$\tau = 1/2^5$	4.7173×10^{-3}	1.02	3579.91	4.7173×10^{-3}	1.02	70.72
$\tau = 1/2^6$	2.3347×10^{-3}	1.01	4622.72	2.3347×10^{-3}	1.01	147.05

Example 2. *The effects of the dynamic parameters on the distributions of velocity and shear force subject to various pressure with cosine forms.*

Figures 3–5 show the distribution of the velocity and shear force at $x = 0$ (wall surface) with oscillating pressure gradient versus time with the form $-\frac{1}{\rho}\frac{\partial p}{\partial z} = \cos(t + 1)$ when we choose $\nu = 1$. The influences of the retardation time parameter on the velocity distributions and the distribution of shear force at the wall are shown in Figure 3. For $\lambda = 0$, the influences of the retardation time disappear. With the appearance of the retardation time parameter, the big difference is that the overall distribution becomes lower with the physical,

meaning that the retardation time parameter reflects a relaxation characteristic in slowing down the velocity propagation and decreasing the magnitude of the shear force at the wall. It can be concluded that a bigger the retardation time parameter corresponds to a larger the relaxation characteristic. The magnetic parameter has important impacts on the distributions of velocity and the shear force. The parameter $M = 0$ indicates that the influence of the magnetic parameter is not considered. As shown in Figure 4, the consideration of the magnetic field makes the distribution at a fixed position smaller, and the value of the distribution becomes smaller when the magnetic parameter becomes bigger. The fractional parameter makes the velocity transport consider the memory characteristic. Figure 5 shows that the value of the distribution becomes smaller with an increase of fractional parameter.
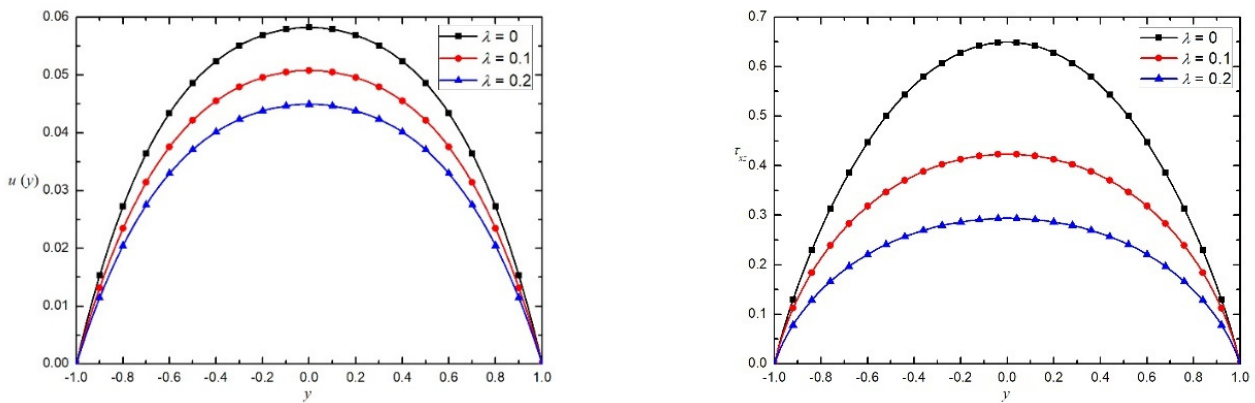
Figure 3. The influences of retardation time parameters on the velocity distribution and the shear force τ_{xz} at the wall surface for $\alpha = 0.5$, $M = 1$ and $-\frac{1}{\rho}\frac{\partial p}{\partial z} = \cos(wt + 1)$.
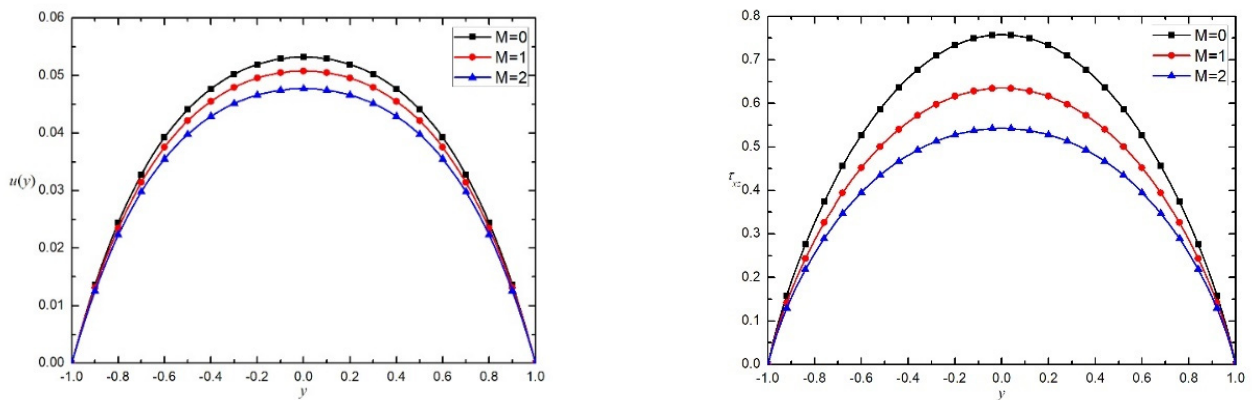
Figure 4. The influences of magnetic parameter on the velocity distribution and the shear force τ_{xz} at the wall surface for $\alpha = 0.5$, $\lambda = 0.1$ and $-\frac{1}{\rho}\frac{\partial p}{\partial z} = \cos(wt + 1)$.

The oscillatory frequency has important impacts on velocity distributions and the shear force distributions. Consider $-\frac{1}{\rho}\frac{\partial p}{\partial z} = \cos(wt + 1)$, the three-dimensional velocity distributions and shear force distributions versus y and t with the effects of frequency are exhibited in Figures 6 and 7, respectively. For $w = 0$, the pressure is constant and the time parameter (for $t > 0$) has no effects on the distributions. For $w \neq 0$, the distributions present as an oscillatory form and the bigger the frequency parameter is, the stronger the oscillatory character of the distributions will be. To discuss the effects of the various pressures with the space oscillatory flow, we consider $-\frac{1}{\rho}\frac{\partial p}{\partial z} = \cos(wz + 1)$ with different w. The effects of frequency parameter on the velocity distributions and the shear force distributions versus x and z are respectively exhibited in Figures 8 and 9. Similarly, the distribution curve shows that the distribution exhibits as a normal form for $w = 0$. For

$w \neq 0$, the distribution presents as an oscillatory form. Finally, the bigger the frequency parameter, the stronger is the oscillation of the distribution curve.
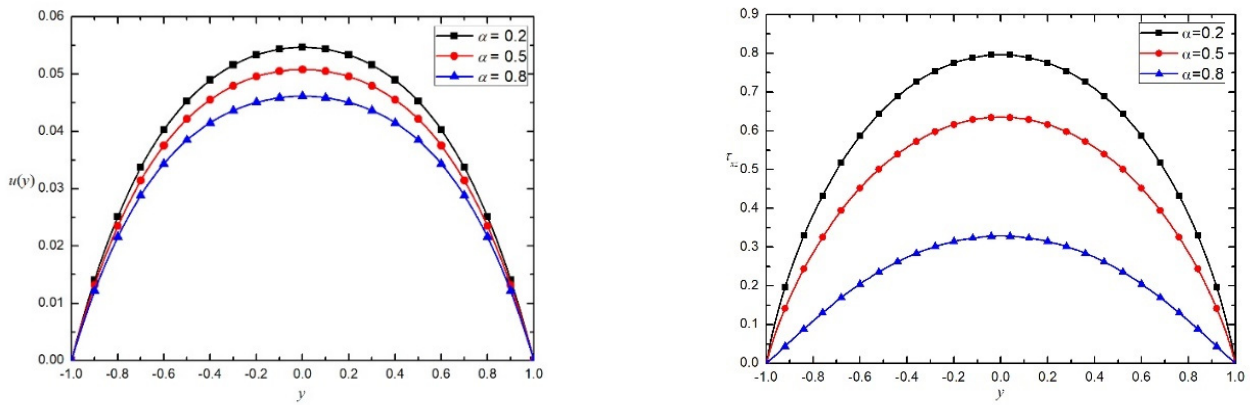
Figure 5. The influences of fractional parameter on the velocity distribution and the shear force τ_{xz} at the wall surface for $M = 1$, $\lambda = 0.1$ and $-\frac{1}{\rho}\frac{\partial p}{\partial z} = \cos(wt + 1)$.
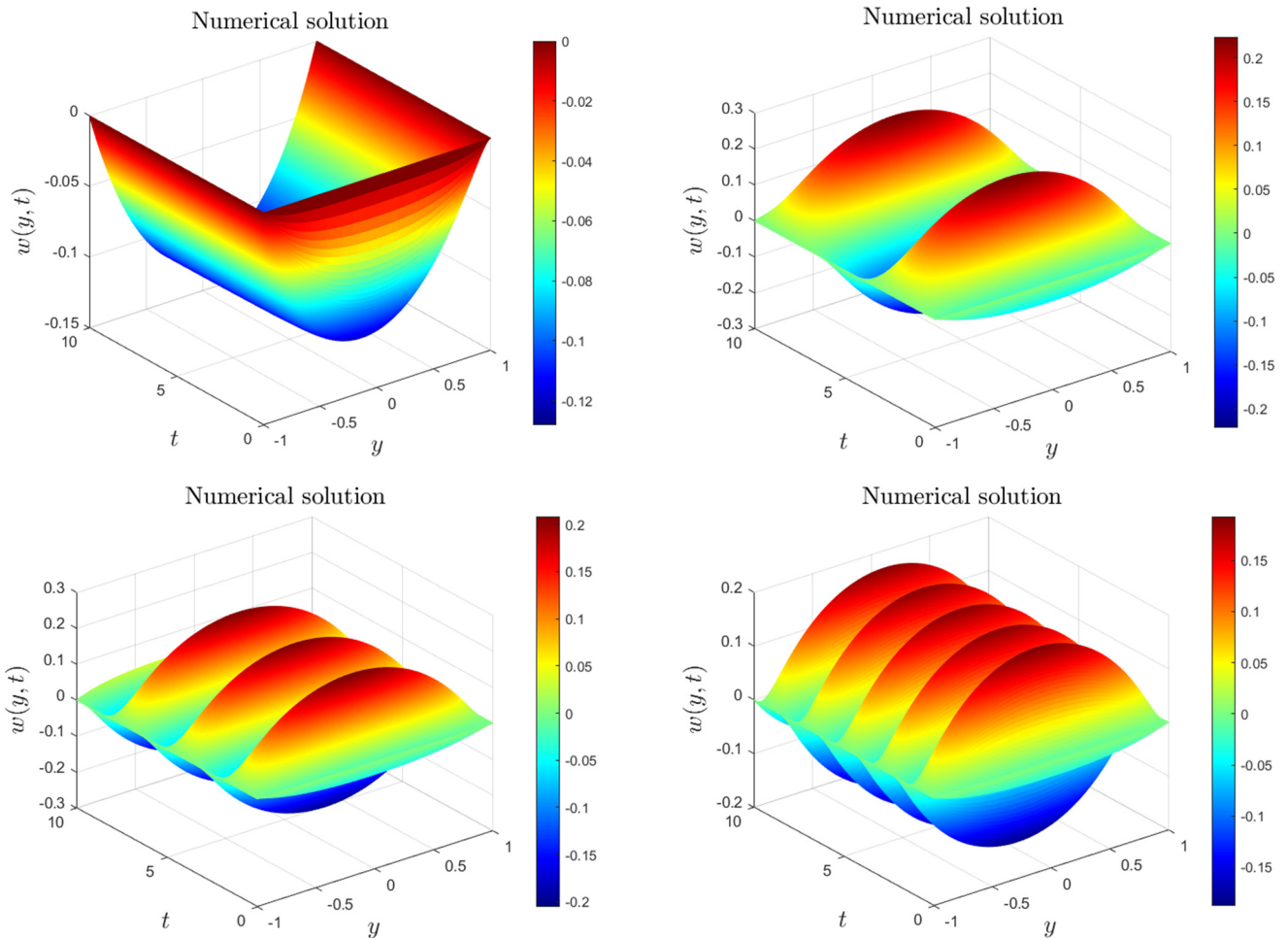
Figure 6. The three-dimensional distribution for velocity field versus y and t with various oscillatory pressure with cosine form versus time $-\frac{1}{\rho}\frac{\partial p}{\partial z} = \cos(wt + 1)$ for different $w = 0, 1, 2, 3$ for $\alpha = 0.5$, $\lambda = 0.1$ and $M = 0.1$.
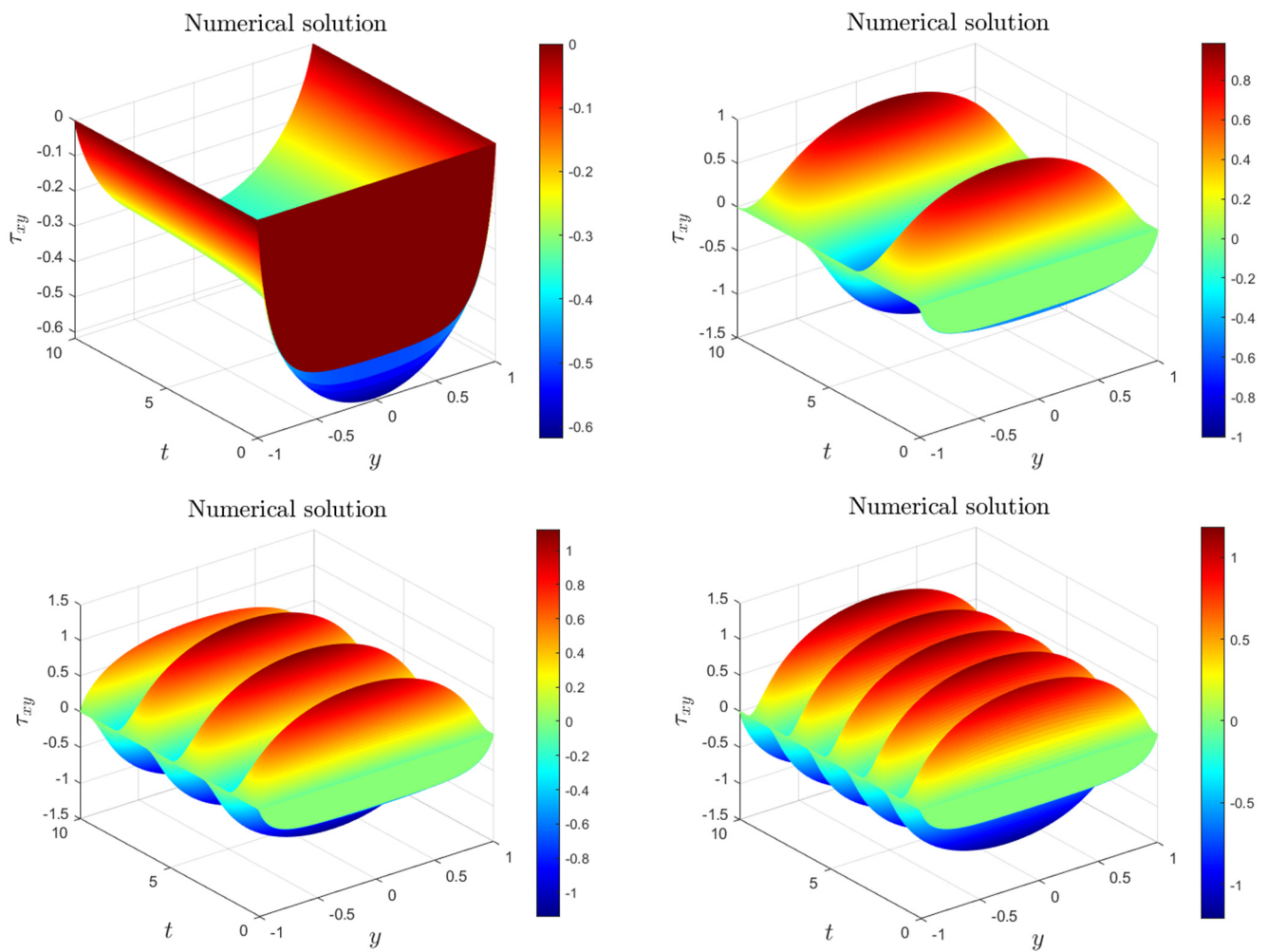
Figure 7. The three-dimensional distribution for shear force versus y and t with various oscillatory pressure with cosine form versus time $-\frac{1}{\rho}\frac{\partial p}{\partial z} = \cos(wt+1)$ for different $w = 0, 1, 2, 3$ for $\alpha = 0.5$, $\lambda = 0.1$ and $M = 1$.
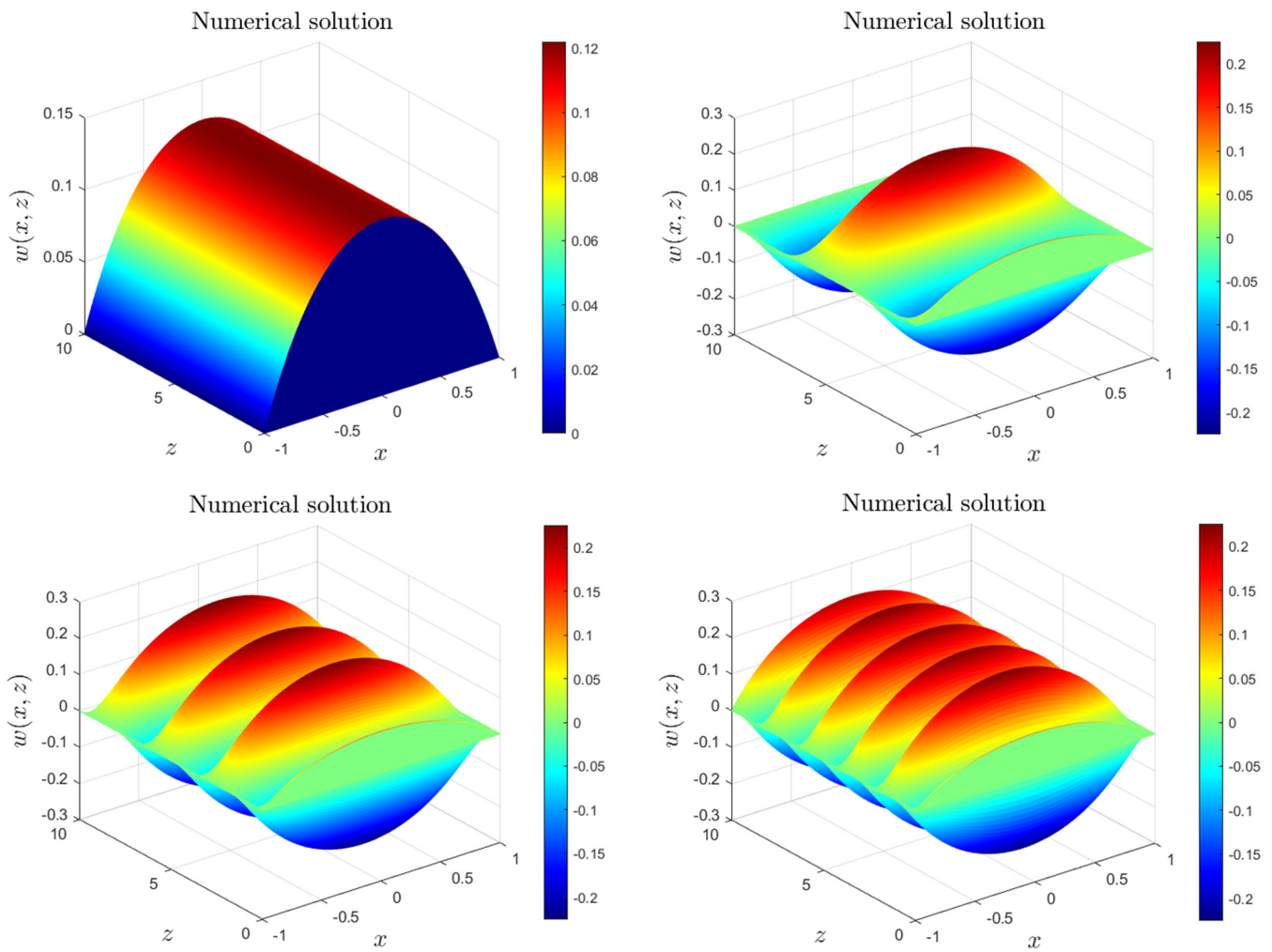
Figure 8. The three-dimensional distribution for velocity versus y and z with various oscillatory pressure with cosine form versus space $-\frac{1}{\rho}\frac{\partial p}{\partial z} = \cos(wz + 1)$ for different $w = 0, 1, 2, 3$ for $\alpha = 0.5$, $\lambda = 0.1$ and $M = 1$.
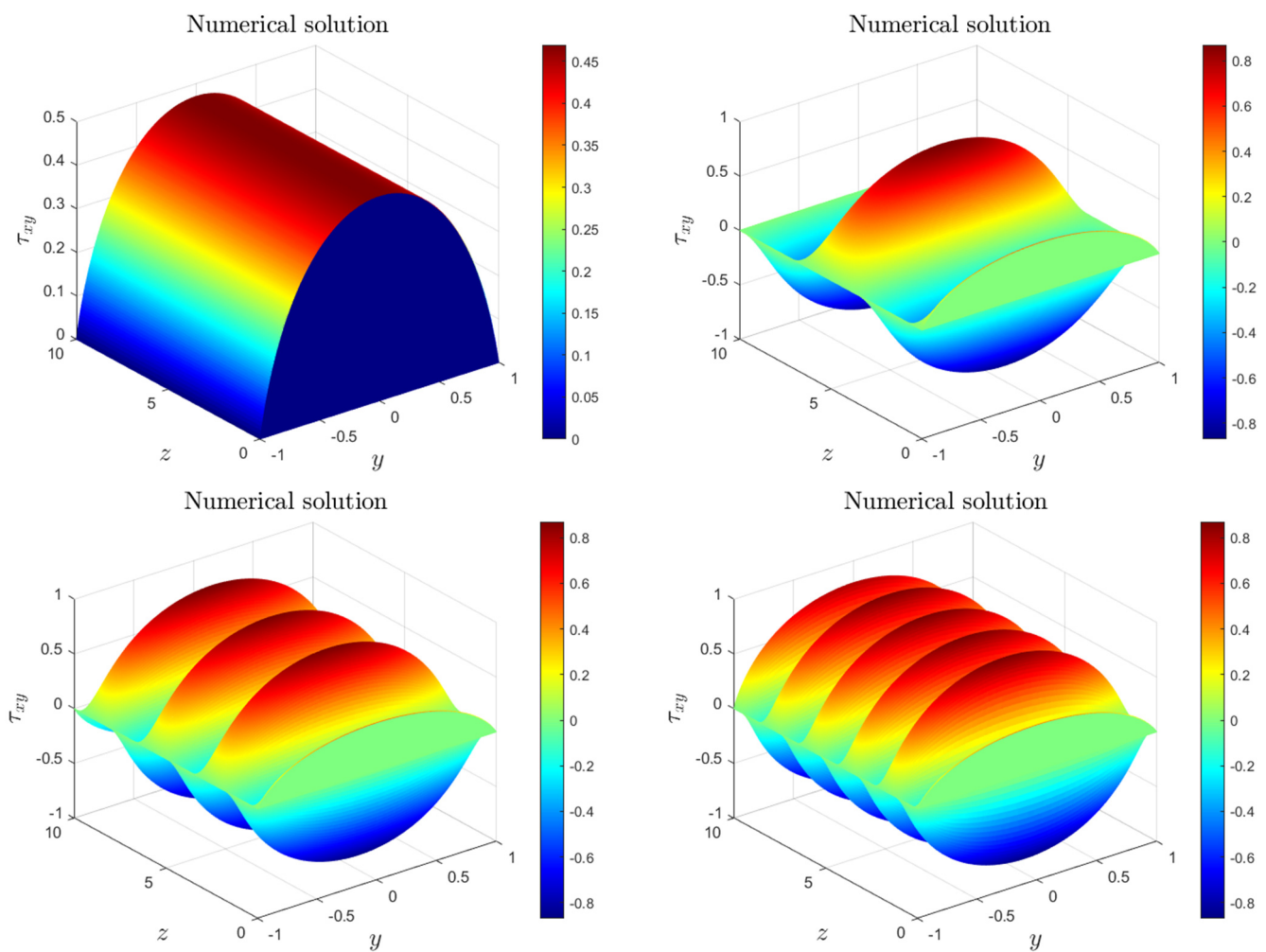
Figure 9. The three-dimensional distribution for shear force versus y and z with various oscillatory pressure with cosine form versus space $-\frac{1}{\rho}\frac{\partial p}{\partial z} = \cos(wz + 1)$ for different $w = 0, 1, 2, 3$ for $\alpha = 0.5$, $\lambda = 0.1$ and $M = 1$.

8. Conclusions

This paper considered the motion of fractional second-grade fluid in a straight rectangular duct. Both the analytical solution and the numerical solution were obtained. For faster computation, a fast scheme was proposed. Two examples were given. One illustrated the accuracy of the numerical solution and the advantage of the fast scheme. The other discussed the impacts of the involved parameters on the velocity distributions and the shear force at the wall surface. The results show that the retardation time parameter plays a role in a relaxation characteristic. The magnetic parameter and fractional parameter with the memory characteristic made the distribution of velocity and shear force become slower. The oscillation of the pressure versus space and time made the distribution present as an oscillatory form and for a larger frequency parameter, the oscillation of the distribution was stronger.

Author Contributions: Conceptualization, L.L. (Lin Liu) and S.C.; methodology, S.Z.; software, J.Z. (Jing Zhu); validation, L.L. (Lang Liu), L.Z. and B.Z.; formal analysis, S.C.; investigation, S.Z.; resources, J.Z. (Jing Zhu); data curation, B.Z.; writing—original draft preparation, B.Z.; writing—review and editing, L.F.; visualization, L.L. (Lang Liu); supervision, L.L. (Lin Liu); project administration, J.Z. (Jiangshan Zhang); funding acquisition, L.L. (Lin Liu). All authors have read and agreed to the published version of the manuscript.

Data Availability Statement: All data reported are obtained by the numerical schemes designed in this paper.

Conflicts of Interest: The authors declare no conflict of interest.

Appendix A

The expanded form of (3) is given as:

$$
A_1 = \nabla V + (\nabla V)^T = \begin{bmatrix} 0 & 0 & 0 \\ 0 & 0 & 0 \\ \frac{\partial w}{\partial x} & \frac{\partial w}{\partial y} & 0 \end{bmatrix} + \begin{bmatrix} 0 & 0 & \frac{\partial w}{\partial x} \\ 0 & 0 & \frac{\partial w}{\partial y} \\ 0 & 0 & 0 \end{bmatrix} = \begin{bmatrix} 0 & 0 & \frac{\partial w}{\partial x} \\ 0 & 0 & \frac{\partial w}{\partial y} \\ \frac{\partial w}{\partial x} & \frac{\partial w}{\partial y} & 0 \end{bmatrix},
$$

$$
\begin{aligned}
A_2 &= D_t^\alpha A_1 + A_1 \nabla V + (\nabla V)^T A_1 \\
&= \begin{pmatrix} 0 & 0 & D_t^\alpha \frac{\partial w}{\partial x} \\ 0 & 0 & D_t^\alpha \frac{\partial w}{\partial y} \\ D_t^\alpha \frac{\partial w}{\partial x} & D_t^\alpha \frac{\partial w}{\partial y} & 0 \end{pmatrix} + \begin{bmatrix} \left(\frac{\partial w}{\partial x}\right)^2 & \frac{\partial w}{\partial x}\frac{\partial w}{\partial y} & 0 \\ \frac{\partial w}{\partial x}\frac{\partial w}{\partial y} & \left(\frac{\partial w}{\partial y}\right)^2 & 0 \\ 0 & 0 & 0 \end{bmatrix} + \begin{bmatrix} \left(\frac{\partial w}{\partial x}\right)^2 & \frac{\partial w}{\partial x}\frac{\partial w}{\partial y} & 0 \\ \frac{\partial w}{\partial x}\frac{\partial w}{\partial y} & \left(\frac{\partial w}{\partial y}\right)^2 & 0 \\ 0 & 0 & 0 \end{bmatrix} \\
&= \begin{pmatrix} 2\left(\frac{\partial w}{\partial x}\right)^2 & 2\frac{\partial w}{\partial x}\frac{\partial w}{\partial y} & D_t^\alpha \frac{\partial w}{\partial x} \\ 2\frac{\partial w}{\partial x}\frac{\partial w}{\partial y} & 2\left(\frac{\partial w}{\partial y}\right)^2 & D_t^\alpha \frac{\partial w}{\partial y} \\ D_t^\alpha \frac{\partial w}{\partial x} & D_t^\alpha \frac{\partial w}{\partial y} & 0 \end{pmatrix}.
\end{aligned}
$$

Then the expression for the shear force is obtained

$$
\begin{aligned}
\tau &= \mu A_1 + \alpha_1 A_2 + \alpha_2 A_1^2 \\
&= \begin{pmatrix} \alpha_1 \left(\frac{\partial w}{\partial x}\right)^2 & \alpha_1 \frac{\partial w}{\partial x}\frac{\partial w}{\partial y} & (\mu + \alpha_1 D_t^\alpha)\frac{\partial w}{\partial x} \\ \alpha_1 \frac{\partial w}{\partial x}\frac{\partial w}{\partial y} & \alpha_1 \left(\frac{\partial w}{\partial y}\right)^2 & (\mu + \alpha_1 D_t^\alpha)\frac{\partial w}{\partial y} \\ (\mu + \alpha_1 D_t^\alpha)\frac{\partial w}{\partial x} & (\mu + \alpha_1 D_t^\alpha)\frac{\partial w}{\partial y} & \alpha_2 \left[\left(\frac{\partial w}{\partial x}\right)^2 + \left(\frac{\partial w}{\partial y}\right)^2\right] \end{pmatrix}
\end{aligned}
$$

References

1. Barna, I.F.; Bognár, G.; Hriczó, K. Self-similar analytic solution of the two dimensional Navier-Stokes equation with a non-Newtonian type of viscosity. *Math. Model. Anal.* **2016**, *21*, 83–94. [CrossRef]
2. Markovitz, H.; Coleman, B.D. Incompressible second-order fluids. *Adv. Appl. Mech.* **1964**, *8*, 69–101.
3. Coleman, B.D.; Noll, W. An approximation theorem for functionals, with applications in continuum mechanics. *Arch. Ration. Mech. Anal.* **1960**, *6*, 355–370. [CrossRef]
4. Kaloni, P.N. Some remarks on "useful theorems for the second order fluid". *J. Non-Newton. Fluid Mech.* **1989**, *31*, 115–120. [CrossRef]
5. Gopalakrishnan, S.S.; Mandal, A.C. Transient growth in a flat plate boundary layer under a stream with uniform shear. *Phys. Fluids* **2022**, *33*, 114101. [CrossRef]
6. Bognár, G. Similarity solution of boundary layer flows for non-Newtonian fluids. *Int. J. Nonlinear Sci. Numer. Simul.* **2009**, *10*, 1555–1566. [CrossRef]
7. Chaves-Guerrero, A.; Peña-Cruz, V.A.; Rinaldi, C.; Fuentes-Díaz, D. Spin-up flow in non-small magnetic fields: Numerical evaluation of the predictions of the common magnetization relaxation equations. *Phys. Fluids* **2017**, *29*, 073102. [CrossRef]
8. Galionis, I.; Hall, P. Stability of the flow in a slowly diverging rectangular duct. *J. Fluid Mech.* **2006**, *555*, 43–58. [CrossRef]
9. Escudier, M.P.; Nickson, A.K.; Poole, R.J. Influence of outlet geometry on strongly swirling turbulent flow through a circular tube. *Phys. Fluids* **2006**, *18*, 125103. [CrossRef]

10. Gao, S.; Hartnett, J.P. Heat transfer behavior of Reiner-Rivlin fluids in rectangular ducts. *Int. J. Heat Mass Transf.* **1996**, *39*, 1317–1324. [CrossRef]

11. Erdoğan, M.E.; İmrak, C.E. Effects of the side walls on the unsteady flow of a second-grade fluid in a duct of uniform cross-section. *Int. J. Non-Linear Mech.* **2004**, *39*, 1379–1384. [CrossRef]

12. Alamri, S.Z.; Khan, A.A.; Azeez, M.; Ellahi, R. Effects of mass transfer on MHD second-grade fluid towards stretching cylinder: A novel perspective of Cattaneo-Christov heat flux model. *Phys. Lett. A* **2018**, *383*, 276–281. [CrossRef]

13. Bernard, J.M. Problem of second-grade fluids in convex polyhedrons. *SIAM J. Math. Anal.* **2012**, *44*, 2018–2038. [CrossRef]

14. Erdoğan, M.E.; İmrak, C.E. On unsteady unidirectional flows of a second-grade fluid. *Int. J. Non-Linear Mech.* **2005**, *40*, 1238–1251. [CrossRef]

15. Wang, X.; Qiao, Y.; Qi, H.; Xu, H. Numerical study of pulsatile non-Newtonian blood flow and heat transfer in small vessels under a magnetic field. *Int. Commun. Heat Mass Transf.* **2022**, *133*, 105930. [CrossRef]

16. Feng, L.; Liu, F.; Turner, I.; Zheng, L. Novel numerical analysis of multi-term time fractional viscoelastic non-Newtonian fluid models for simulating unsteady MHD Couette flow of a generalized Oldroyd-B fluid. *Fract. Calc. Appl. Anal.* **2018**, *21*, 1073–1103. [CrossRef]

17. Brunner, H.; Ling, L.; Yamamoto, M. Numerical simulations of 2D fractional subdiffusion problems. *J. Comput. Phys.* **2010**, *229*, 6613–6622. [CrossRef]

18. Feng, C.; Li, B.; Si, X.; Wang, W.; Zhu, J. The electro-osmotic flow and heat transfer of generalized Maxwell fluids with distributed-order time-fractional characteristics in microtubules under an alternating field. *Phys. Fluids* **2021**, *33*, 113105. [CrossRef]

19. Feng, L.; Liu, F.; Turner, I.; Zhuang, P. Numerical methods and analysis for simulating the flow of a generalized Oldroyd-B fluid between two infinite parallel rigid plates. *Int. J. Heat Mass Transf.* **2017**, *115*, 1309–1320. [CrossRef]

20. Khan, M.; Anjum, A.; Fetecau, C.; Qi, H. Exact solutions for some oscillating motions of a fractional Burgers' fluid. *Math. Comput. Model.* **2010**, *51*, 682–692. [CrossRef]

21. Tan, W.; Xu, M. The impulsive motion of flat plate in a generalized second-grade fluid. *Mech. Res. Commun.* **2002**, *29*, 3–9. [CrossRef]

22. Bazhlekova, E.; Jin, B.; Lazarov, R.; Zhou, Z. An analysis of the Rayleigh-Stokes problem for a generalized second-grade fluid. *Numer. Math.* **2015**, *131*, 1–31. [CrossRef] [PubMed]

23. Khan, M.; Wang, S. Flow of a generalized second-grade fluid between two side walls perpendicular to a plate with a fractional derivative model. *Nonlinear Anal. Real World Appl.* **2009**, *10*, 203–208. [CrossRef]

24. Li, J.; Si, X.; Li, B.; Cao, L.; Zhang, P. The effects of depletion layer for electro-osmotic flow of fractional second-grade viscoelastic fluid in a micro-rectangle channel. *Appl. Math. Comput.* **2020**, *385*, 125409. [CrossRef]

25. Sun, X.; Wang, S.; Zhao, M. Oscillatory flow of Maxwell fluid in a tube of isosceles right triangular cross section. *Phys. Fluids* **2019**, *31*, 123101.

26. Xu, H.; Wang, S.; Zhao, M. Oscillatory flow of second-grade fluid in a straight rectangular duct. *J. Non-Newton. Fluid Mech.* **2020**, *279*, 104245. [CrossRef]

27. Fetecau, C.; Hayat, T.; Fetecau, C. Starting solutions for oscillating motions of Oldroyd-B fluids in cylindrical domains. *J. Non-Newton. Fluid Mech.* **2008**, *153*, 191–201. [CrossRef]

28. Fetecau, C.; Hayat, T.; Khan, M.; Fetecau, C. A note on longitudinal oscillations of a generalized Burgers fluid in cylindrical domains. *J. Non-Newton. Fluid Mech.* **2010**, *165*, 350–361. [CrossRef]

29. Manzini, G. An efficient and conservative hybrid method for solving multi-dimensional conservation laws. *Numer. Methods Partial. Diff. Eqs.* **2009**, *25*, 1029–1066. [CrossRef]

30. Harris, P.A.; Garra, R. Nonlinear time-fractional dispersive equations. *Commun. Appl. Ind. Math.* **2014**, *6*, e487.

31. Barna, I.F.; Mátyás, L. Advanced Analytic Self-Similar Solutions of Regular and Irregular Diffusion Equations. *Mathematics* **2022**, *10*, 3281. [CrossRef]

32. Khan, M.; Fetecau, C.; Hayat, T. MHD transient flows in a channel of rectangular cross-section with porous medium. *Phys. Lett. A* **2007**, *369*, 44–54. [CrossRef]

33. Nadeem, S.; Asghar, S.; Hayat, T.; Hussain, M. The rayleigh stokes problem for rectangular pipe in maxwell and second-grade fluid. *Meccanica* **2008**, *43*, 495–504. [CrossRef]

34. Christov, I.C. Stokes first problem for some non-Newtonian fluids: Results and mistakes. *Mech. Res. Commun.* **2010**, *37*, 717–723. [CrossRef]

35. Christov, I.C. On a difficulty in the formulation of initial and boundary conditions for eigenfunction expansion solutions for the start-up of fluid flow. *Mech. Res. Commun.* **2013**, *51*, 86–92. [CrossRef]

36. Majak, J.; Shvartsman, B.; Pohlak, M.; Karjust, K.; Eerme, M.; Tungel, E. Solution of fractional order differential equation by the Haar Wavelet method. Numerical convergence analysis for most commonly used approach. *AIP Conf. Proc.* **2016**, *1738*, 480110.

37. Sun, Z.; Wu, X. A fully discrete difference scheme for a diffusion-wave system. *Appl. Numer. Math.* **2006**, *56*, 193–209. [CrossRef]

38. Jiang, S.; Zhang, J.; Zhang, Q.; Zhang, Z. Fast evaluation of the Caputo fractional derivative and its applications to fractional diffusion equations. *Commun. Comput. Phys.* **2015**, *21*, 650–678. [CrossRef]

39. Yan, Y.; Sun, Z.; Zhang, J. Fast evaluation of the Caputo fractional derivative and its applications to fractional diffusion equations: A second-order scheme. *Commun. Comput. Phys.* **2017**, *22*, 1028–1048. [CrossRef]

40. Gao, G.; Yang, Q. Fast evaluation of linear combinations of caputo fractional derivatives and its applications to multi-Term time-fractional sub-diffusion equations. *Numer. Math. Theory Methods Appl.* **2020**, *13*, 433–451.
41. Lyu, P.; Liang, Y.; Wang, Z. A fast linearized finite difference method for the nonlinear multi-term time-fractional wave equation. *Appl. Numer. Math.* **2020**, *151*, 448–471. [CrossRef]
42. Ran, M.; Lei, X. A fast difference scheme for the variable coefficient time-fractional diffusion wave equations. *Appl. Numer. Math.* **2021**, *167*, 31–44. [CrossRef]
43. Podlubny, I. *Fractional Differential Equations*; Academic Press: New York, NY, USA, 1999.
44. Dunn, J.E.; Fosdick, R.L. Thermodynamics, stability, and boundedness of fluids of complexity 2 and fluids of second-grade. *Arch. Ration. Mech. Anal.* **1974**, *56*, 191–252. [CrossRef]
45. Dunn, J.E.; Rajagopal, K.R. Fluids of differential type: Critical review and thermodynamic analysis. *Int. J. Eng. Sci.* **1995**, *33*, 689–729. [CrossRef]
46. Shen, S.; Liu, F.; Anh, V.V. The analytical solution and numerical solutions for a two-dimensional multi-term time fractional diffusion and diffusion-wave equation. *J. Comput. Appl. Math.* **2019**, *345*, 515–534. [CrossRef]
47. Neudecker, H. A note on kronecker products and matrix equation systems. *SIAM J. Appl. Math.* **1969**, *17*, 603–606. [CrossRef]
48. Berardi, M.; Difonzo, F.V. A quadrature-based scheme for numerical solutions to Kirchhoff transformed Richards' equation. *J. Comput. Dyn.* **2022**, *9*, 69–84. [CrossRef]
49. Horn, R.A.; Johnson, C.R. *Topics in Matrix Analysis*; Cambridge University Press: Cambridge, UK, 1994.
50. Fu, H.; Liu, H.; Wang, H. A finite volume method for two-dimensional Riemann-Liouville space-fractional diffusion equation and its efficient implementation. *J. Comput. Phys.* **2019**, *388*, 316–334. [CrossRef]
51. Sun, H.; Sun, Z. A fast temporal second-order compact ADI difference scheme for the 2D multi-term fractional wave equation. *Numer. Algorithms* **2021**, *86*, 761–797. [CrossRef]